Sensitivity of force-detected NMR spectroscopy with resonator-induced polarization

Mark C. Butler* and Daniel P. Weitekamp

A. A. Noyes Laboratory of Chemical Physics, California Institute of Technology, MC 127-72, Pasadena, California 91125, USA

(Received 19 August 2012; published 13 February 2013)

In the low-temperature regime where the thermal polarization P is of order unity and spin-lattice relaxation is "frozen out," resonator-induced relaxation can be used to polarize a nuclear-spin sample for optimal detection sensitivity. We characterize the potential of resonator-induced polarization for enhancing the sensitivity of nuclear-magnetic-resonance spectroscopy. The sensitivities of two detection schemes are compared, one involving detection of a polarized sample dipole and the other involving detection of spin-noise correlations in an unpolarized sample. In the case where the dominant noise source is instrument noise associated with resonator fluctuations and with detection of the mechanical motion, a simple criterion can be used to compare the two schemes. Polarizing the sample improves sensitivity when P is larger than the signal-to-noise ratio for detection of a fully-polarized spin during a single transient. Even if the instrument noise is decreased to a level near the quantum-mechanical limit, it is larger than spin noise for unpolarized samples containing up to a few tens of nuclei. Under these conditions, spin polarization of order unity would enhance spectroscopic detection sensitivity by an order of magnitude or more. In the limiting case where signal decay is due to resonator-induced dissipation during ideal spin locking, and where resonator fluctuations are the noise source, the only parameter of the spin-resonator system that affects the sensitivity per spin is the ratio of frequency to temperature. A balance between the coupling strength, the noise power, and the signal lifetime causes the cancellation of other parameters from the sensitivity formula. Partial cancellation of parameters, associated with a balance between the same three quantities, occurs more generally when the resonator is both the dominant noise source and the dominant source of signal decay. An intrinsic sensitivity limit exists for resonant detection of coherent spin evolution, due to the fact that the detector causes signal decay by enhancing the spins' spontaneous emission. For a single-spin sample, the quantum-limited signal-to-noise ratio for resonant detection is $1/3$. In contrast to the sensitivity, the time required for sample polarization between transients depends strongly on resonator parameters. We discuss resonator design and show that for a torsional resonator, the coupling is optimal when the resonator's magnetization remains aligned with the applied field during the mechanical oscillations.

DOI: 10.1103/PhysRevB.87.064413 PACS number(s): 76.60.−k, 82.56.−b, 33.25.+k, 37.10.−x

I. INTRODUCTION

Force-detected nuclear magnetic resonance (NMR) has emerged in recent years as a sensitive tool for the study of microscopic spin samples. The sensitivity of magnetic-resonance force microscopy (MRFM)[1–3] has increased by approximately seven orders of magnitude in the 20 years since MRFM experiments were reported,[1] enabling nuclear-spin imaging with a resolution better than 10 nm.[4] MRFM detectors have been used for spatially-localized NMR spectroscopy, including the detection of dipolar evolution,[5] chemical shifts,[6] double resonance,[7,8] and quadrupolar nutation.[9] Force-detected NMR without the use of field gradients (BOOMERANG)[10] has been demonstrated by the spectroscopic measurement of scalar couplings.[11]

One of the goals inspiring the development of force-detected NMR is signal detection with single-spin sensitivity.[12] In samples containing a small number of spins, signal detection is complicated by the fact that the uncertainty in the sample dipole is large compared to the mean dipole unless the polarization is of order unity. At the millikelvin temperatures needed to achieve this level of thermal polarization in a magnetic field of several teslas, the spin-lattice relaxation that restores polarization between transients becomes inconveniently slow,[13] making signal averaging impractical. Resonator-induced relaxation has been proposed as a means of returning spins to thermal equilibrium between transients,[14] and a calculation based on a prototypical resonator design suggests that relaxation of nanoscale samples to polarization of order unity with a rate constant $R_h \sim 1\ \mathrm{s}^{-1}$ may be possible at millikelvin temperatures.[15]

An alternative to restoring thermal polarization between transients is to detect spin noise. MRFM methods based on the measurement of spin noise[16] have been used for nuclear-spin imaging of nanoscale samples,[4] detection of double resonance,[7] and detection of a single electron spin.[17] Magnetic-resonance spectra of alkali-metal atoms have been measured by optical detection of correlations in spin noise,[18] and NMR spectra of liquids and solids have been obtained by detecting spin noise with a tuned circuit.[19] A method of encoding NMR spectra into correlated measurements of spin noise has been proposed (CONQUEST).[20–22]

Although the record of sensitivity improvements for MRFM methods is impressive, the achievement of single-proton sensitivity remains a very challenging problem, requiring an improvement of two orders of magnitude in sensitivity.[1] BOOMERANG methods include a scheme for achieving single-proton sensitivity,[15] based on the use of a torsional resonator to detect spin precession[11] and restore thermal polarization between transients. In contrast to MRFM, where sensitive detection depends on the presence of a large field gradient,[1] detectors for BOOMERANG are designed to yield a homogeneous field at the sample. A homogeneous field facilitates coherent manipulation of the entire spin system and maximizes the sensitivity of both spectroscopy and imaging

by allowing each shot to include signal from the entire sample.[10] BOOMERANG is also promising for combining force detection with resonator-induced polarization, since polarization of the entire sample rather than a resonant slice is possible when the field is homogeneous.[14]

The work presented here characterizes the potential of resonator-induced polarization for enhancing the sensitivity of force-detected NMR spectroscopy. In Sec. II, we derive signal-to-noise-ratio formulas for two spectroscopic detection schemes, one involving detection of a polarized sample dipole and the other involving detection of spin-noise correlations in an unpolarized sample. Our attention is centered on the case where the thermal number of quanta in the resonator is small and the effective sample volume contains up to a few tens of nuclear spins, but the derived results are valid outside of this regime. When the dominant noise source is instrument noise associated with resonator fluctuations and with detection of the mechanical motion, the relative sensitivity of the two detection schemes is shown to be P^2N/ρ, where P is the thermal polarization, N is the number of spins, and ρ is the single-shot signal-to-noise ratio (SNR) for detection of the thermally-polarized sample dipole. If P is larger than the SNR for detection of a fully-polarized spin during a single transient, sample polarization improves spectroscopic sensitivity. Even if instrument noise is decreased to a level near the quantum-mechanical limit, it is larger than spin noise for samples containing up to a few tens of unpolarized nuclei. Under these conditions, spin polarization of order unity would enhance spectroscopic detection sensitivity by an order of magnitude or more over the sensitivity attainable by detection of spin-noise correlations.

A strong spin-resonator coupling that yields fast thermal relaxation between transients can also shorten the signal lifetime.[23] Section III examines the way in which resonator-induced signal decay affects sensitivity. Relaxation during pulsed spin locking is first characterized. Averaging of the resonator-induced transitions requires nutation of the entire spin system about the spin-locking field, which in turn requires a field sufficiently strong to average the internal spin Hamiltonian $H_{\rm int}$. As in the case of continuous spin locking,[23] effective averaging during pulsed spin locking yields a signal that is damped exponentially with time constant $T_{1\rho} = 2/R_h$, where R_h is the rate constant for resonator-induced polarization in the absence of the applied rf field.

In the case where spin noise is negligible, and where the noise associated with the motion detector is equivalent to a fixed number of thermal quanta added to the resonator, we obtain a surprising simplification of the sensitivity formula for detection during ideal spin locking. The sensitivity per spin depends on the properties of the spin-resonator system through only a single parameter: the ratio of frequency to temperature. The cancellation of parameters from the sensitivity formula is due to a balance between the coupling strength, the noise power of the resonator's fluctuations, and the signal lifetime, which is shortened by resonator-induced dissipation. Partial cancellation of parameters, associated with a balance between the same three quantities, occurs more generally when the resonator is both the dominant noise source and the dominant source of signal decay. An intrinsic sensitivity limit exists for resonant detection of coherent spin evolution, due to the fact that the resonant interaction enhances the spins' spontaneous emission. For quantum-limited detection, signal decay is due to the spontaneous emission of individual spins into the resonant mode and the SNR for detection of a single spin is 1/3. Formally, the limit on detection sensitivity can be shown to exist when the detector is a damped harmonic oscillator whose resonant interaction with the spins is governed by the Jaynes-Cummings Hamiltonian,[24] with the coupling sufficiently weak that the detector perturbs the spin evolution only by causing signal decay. Physical examples include Rydberg atoms coupled to a damped cavity mode[25] and nuclear spins coupled to a tuned circuit[14] or a mechanical resonator.

The time required for polarization between transients is minimized when the resonator has a small motional mass and a strong coupling to the spins and when the friction that damps the resonator's response to the spins is weak. For a torsional resonator, the coupling does not depend on a gradient generated by the resonator's magnets or on relative motion between the magnets and the sample. This form of coupling is advantageous for spin polarization and NMR spectroscopy, because it allows for designs that optimize field homogeneity and place the resonator's magnets arbitrarily close to the sample, without the problem of friction due to relative motion between the magnets and the sample.[15] Section IV discusses resonator design and shows that, for a torsional resonator, the coupling strength is enhanced when the resonator's magnetization remains aligned with the applied field during the mechanical oscillations. Order-of-magnitude estimates are used to characterize the experimental regime relevant for NMR spectroscopy with resonator-induced polarization. For single molecules with resolved one-dimensional spectra, direct detection of free evolution is possible, with signal lifetime limited by resonator-induced dissipation and radiation damping. For larger samples, where free evolution yields a short-lived signal, pulsed spin locking during the detection period optimizes the sensitivity of multidimensional methods in which information is encoded into an arbitrary evolution period before detection.

II. SENSITIVITY ANALYSIS

The sensitivity of force-detected magnetic resonance has been studied in detail. In particular, the sensitivities of force detection and inductive detection have been compared,[10,26] the factors that determine the SNR of MRFM[1–3] and BOOMERANG[10] have been analyzed, and the sensitivities of MRFM methods based on spin-noise detection have been characterized.[16] In the current discussion, we compare the sensitivities of two spectroscopic detection schemes in the regime where the number of thermal quanta in the resonator is small and the sample contains up to a few tens of nuclei. SNR formulas are derived and used to characterize the conditions under which polarization improves spectroscopic sensitivity.

Figure 1 shows a prototypical design for a torsional resonator, previously proposed for the polarization and spectroscopy of low-temperature nanoscale samples.[15] We use this resonator design for purposes of illustration and define notation based on Fig. 1, but most of the analysis is not substantially

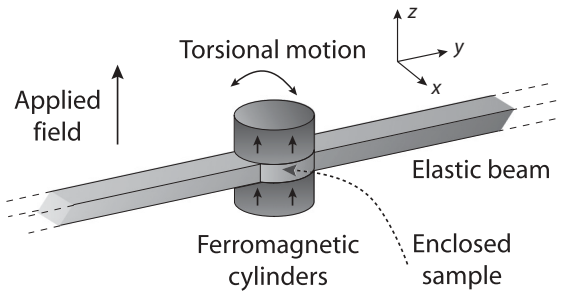

FIG. 1. Prototypical resonator design proposed in Ref. 15 for NMR spectroscopy of nanoscale samples. The sample is "sandwiched" between magnetic cylinders and rotates with the sandwich about the torsional beam. The spin dipole couples to the oscillating transverse field generated by the cylinders.

altered if this resonator is replaced with a translational mechanical resonator whose motion is coupled through its field gradient to the Larmor precession of the spins. (Results that depend specifically on the use of a torsional resonator are presented in Sec. IV.) The figure shows a "magnetic sandwich" that consists of two ferromagnetic cylinders and a disk of silicon that separates them, with the sample placed in a hollow space in the center of the silicon disk. The sandwich encloses the center of an elastic beam, and the beam and sandwich together undergo torsional oscillations about the beam's long axis, labeled as the y axis in the figure. The structure consisting of the sandwich and the beam is a torsional mechanical oscillator with fundamental frequency ω_h and coordinate θ, defined as the angular displacement of the sandwich axis from the z axis. Since the motion of the ferromagnetic cylinders modulates the magnetic field $\mathbf{B}(\theta)$ at the spins, the oscillator is coupled to the spins, and the coupling does not depend on the presence of a field gradient at the sample.

To first order in θ, only the field component B_x is modulated by the mechanical motion.[14] The oscillating transverse field component induces spin transitions if ω_h is resonant with the Larmor frequency ω_0, and these transitions can polarize the spins[14] or cause dissipation of transients.[23] The resonator can also serve as a detector, since a precessing sample dipole exerts a resonant torque that drives mechanical motion. The interaction between the spin sample and the resonator is governed by the potential energy

$$W = -\boldsymbol{\mu} \cdot \mathbf{B}(\theta),$$

where $\boldsymbol{\mu} = \gamma\hbar\mathbf{I}$ is the sample dipole, with γ the gyromagnetic ratio and $\mathbf{I}$ the spin operator, summed over the spins. Approximating $\mathbf{B}(\theta)$ to first order in θ, we find that the torque exerted by the spins is

$$-\frac{\partial W}{\partial \theta} = \gamma\hbar \frac{dB_x}{d\theta} I_x. \tag{1}$$

This torque rotates the sandwich, pulling its axis toward alignment with I_x. In a conventional inductive spectrometer, magnetization in the transverse plane similarly exerts a torque on the coils that generate the static field, but the torque is of no consequence because the coils are massive and fixed in place.

A. Detection of a polarized dipole

1. Detection scheme

We first consider a detection scheme in which the spins are polarized at the beginning of each transient, with resonator-induced polarization replacing spin-lattice relaxation as a means of restoring polarization between transients.[14] For simplicity, the polarization at the beginning of each transient is assumed to equal the equilibrium value for spins 1/2:

$$P = \tanh\left(\frac{\hbar\omega_h}{2k_B T_h}\right). \tag{2}$$

In Eq. (2), T_h is the temperature of the thermal bath that cools the resonator. Note that the polarization process depends on the resonance condition $\omega_h = |\omega_0|$, and we typically express equations in terms of ω_h rather than ω_0.

In the BOOMERANG detection scheme,[10,11] a conventional NMR pulse sequence is applied to the spins, which then evolve freely during a period t_1, corresponding to the initial part of a free-induction decay (FID). The FID is terminated by application of rf fields that manipulate the spins and cause the sample dipole to oscillate at the mechanical frequency, so that the spins drive mechanical motion. In the present case, where the mechanical motion is resonant with Larmor precession, this spin manipulation can be implemented by means of pulsed spin locking.[27,28] Between pulses, the resonator responds to the driving torque exerted by the spin-locked component. Detection and analysis of the resulting mechanical motion yields a measurement of $\langle I_x \rangle (t_1)$, which corresponds to a single point on the FID. A record of the spins' time evolution during the FID is obtained by repeating this measurement for a range of values t_1, and Fourier analysis yields the NMR spectrum. An additional feature of the detection scheme is the possibility of shifting the spins out of resonance with the mechanical oscillator during the period of spectral evolution in order to eliminate modifications to the line shape associated with a strong resonant coupling to the oscillator.[15]

Pulsed spin locking has previously been used as a means of enhancing signal energy in inductively detected experiments.[29–32] The resulting increase in sensitivity has been characterized in the contexts of multiple-quantum spectroscopy,[29] indirect detection of heteronuclei,[31] and structural measurements based on dipolar recoupling and chemical-shift anisotropy.[32] For the freely evolving system, the energy of the signal is proportional to the time constant T_2^* for signal decay, while pulsed spin locking yields a signal energy proportional to $DT_{1\rho}$, where D and $T_{1\rho}$ are the duty cycle of the detector and the time constant for signal decay during pulsed spin locking, respectively. The sensitivity enhancement associated with pulsed spin locking is thus $\propto\sqrt{DT_{1\rho}/T_2^*}$.[10] In the regime of interest for the current discussion, T_2^* can be shortened by resonator-induced dissipation and radiation damping, as well as by dephasing under the internal spin Hamiltonian $H_{\rm int}$. As discussed in Sec. III A, nutation of the entire spin system about the spin-locking field averages both the resonator-induced transitions and the evolution governed by $H_{\rm int}$, which yields a signal lifetime $T_{1\rho} = 2/R_h$, where R_h is the rate constant for resonator-induced polarization between transients.

2. *Instrument noise*

In analyzing the sensitivity of the BOOMERANG detection scheme, we initially neglect the duty cycle and assume that continuous observation of a torsional resonator yields a measured coordinate $\theta_{\rm obs}(t)$. The noise in $\theta_{\rm obs}$ is

$$\delta\theta(t) = \theta_{\rm obs}(t) - \langle\theta(t)\rangle\,,$$

where $\langle\theta(t)\rangle$ is the statistical average over an ensemble of spin-resonator systems. Note that $\langle\theta(t)\rangle$ carries information about the driving torque exerted by the polarized sample dipole, while $\delta\theta(t)$ depends on spin fluctuations, mechanical fluctuations, and noise associated with the detection of the mechanical motion.

It is convenient to define the signal as a torque exerted on the resonator by the spins, since for small mechanical displacements, the torque at time t is determined by the instantaneous spin state and does not depend on the resonator's previous motion. Our sensitivity analysis is based on an idealized signal-processing scheme, discussed in Appendix A 1, and this scheme can be considered to include a calculation of the torque $T_{\rm obs}(t)$ needed to produce an expected displacement of $\theta_{\rm obs}(t)$ in the resonator.

We begin the analysis by considering the quantum Langevin equation[33] for the Heisenberg operator $\theta(t)$:

$$I_h\frac{d^2}{dt^2}\theta(t) + \frac{2I_h}{\tau_h}\frac{d}{dt}\theta(t) + k_h\theta(t) = T(t) + N_{\rm th}(t). \quad (3)$$

In Eq. (3), I_h is the resonator's moment of inertia, τ_h is the time constant for decay of the mechanical displacement, k_h is the torsional spring constant, $N_{\rm th}(t)$ is a fluctuating torque associated with the thermal bath, and

$$T(t) = \gamma\hbar\frac{dB_x}{d\theta}I_x(t) \quad (4)$$

is the torque exerted on the resonator by the spins. The field $\mathbf{B}(\theta)$ has been approximated to first order in θ, as in Eq. (1). The derivation of Eq. (3) is similar to the derivation of the quantum Langevin equation for a particle moving in an external potential.[34]

The signal torque $s(t)$ is given by the expectation value of $T(t)$:

$$s(t) = \gamma\hbar\frac{dB_x}{d\theta}\langle I_x(t)\rangle\,. \quad (5)$$

Taking the statistical average of both sides of Eq. (3) shows that the motion of $\langle\theta(t)\rangle$ is driven by $s(t)$, since $\langle N_{\rm th}(t)\rangle = 0$.

The spectral density of $N_{\rm th}(t)$ can be derived from an analysis of the Langevin equation,[34] or by means of the quantum regression formula,[35] which can be used to characterize the driven oscillator's fluctuations. The single-sided spectral density is

$$S_N(\omega) = \frac{8I_h}{\tau_h}\hbar\omega\left[n_{\rm th}(\omega) + \frac{1}{2}\right], \quad (6)$$

where

$$n_{\rm th}(\omega) = \frac{1}{\exp(\hbar\omega/k_BT_h) - 1}$$

is the number of thermal quanta in a harmonic oscillator of frequency ω at temperature T_h. To simplify notation, we drop the frequency argument from $n_{\rm th}$ and from noise spectral densities when $\omega = \omega_h$.

If the temperature is sufficiently low that the $P \sim 1$, the resonator's zero-point motion makes a non-negligible contribution to the mechanical fluctuations, since

$$n_{\rm th} = \frac{1}{2}\left(\frac{1}{P} - 1\right). \quad (7)$$

In this regime, quantum mechanics imposes a limitation on the accuracy with which $\langle\theta(t)\rangle$ can be measured.[36,37] Quantum-limited detection of the mechanical motion occurs when the noise added by the detector is equivalent to the noise resulting from the torque $N_{\rm th}$ at temperature $T_h = 0$ K.[36] For quantum-limited motion detection, the spectral density of the instrument noise associated with resonator fluctuations and with motion detection is

$$S_{\rm inst}(\omega) = \frac{8I_h}{\tau_h}\hbar\omega\left[n_{\rm th}(\omega) + 1\right]. \quad (8)$$

Note that in moving from Eq. (6) to Eq. (8), we have doubled the contribution to the spectral density associated with the resonator's zero-point motion.

Nonideal motion detection would conventionally be characterized in terms of a noise temperature T_n, which expresses the noise added by the detector in terms of an equivalent increase in the resonator temperature. Since T_n depends on the resonator temperature, rather than being determined by the properties of the detector itself, differing conventions exist for the definition of T_n.[36] A convenient alternative to the use of a noise temperature is to characterize nonideal detection in terms of the noise number A, defined as the increase in the resonator's thermal quanta needed to account for the detector noise.[37] For nonideal motion detection, we have

$$S_{\rm inst}(\omega) = \frac{8I_h}{\tau_h}\hbar\omega\left[n_{\rm th}(\omega) + \frac{1}{2} + A\right]. \quad (9)$$

In the regime considered here, where the bandwidth of resonator fluctuations is broad compared to the signal bandwidth, the use of Eq. (9) amounts to an assumption that the motion detector adds white noise to the measured coordinate $\theta_{\rm obs}(t)$.

The variance introduced into the measurement by instrument noise depends on the effective bandwidth of the measurement. For the signal-processing protocol described in Appendix A 1, which is based on the use of a matched filter to analyze the data, the bandwidth is

$$\Delta\nu = \frac{2}{DT_{1\rho}},$$

and the variance associated with filtered instrument noise is given by Eq. (A16) as

$$\sigma^2_{\rm inst} = \frac{2}{DT_{1\rho}}S_{\rm inst}. \quad (10)$$

Note that Eq. (10) takes account of the loss of signal energy associated with the fact that the resonator can only function as a detector during a fraction D of the detection period.

3. *Spin noise*

The torque exerted on the resonator by the spins is described by the operator $T(t)$ of Eq. (4), and uncertainty associated

with this operator introduces noise into the measurement. Physically, this noise source can be identified with spin fluctuations. An analysis of the power spectrum of these fluctuations is not straightforward, since they cannot, in general, be described as a stationary random process. For example, the bandwidth of the spin fluctuations depends on the time constants for spin relaxation, and these are affected by the presence of the spin-locking field. The fluctuations occurring during the detection period thus differ from those occurring during the preceding period of free evolution, and a detailed description of the frequency components of the spin noise would need to take account of this fact.

Another complicating factor is that spin fluctuations depend on the spin state, which changes during the measurement process. A simple example, discussed in greater detail in Sec. III B, illustrates this. Consider a single-spin sample that is polarized by a resonator at 0 K and then detected during a period of free precession, with signal decay caused by the spin's spontaneous emission into the resonator. The spin is aligned with the x axis at the beginning of the detection period, and so the initial uncertainty in the spin torque $T(t) \propto I_x(t)$ is zero. However, shot-to-shot variation in the duration of the transient due to spontaneous emission constitutes a form of spin noise, since it is associated with fluctuations away from $\langle I_x(t)\rangle$. The spin noise therefore evolves during the detection period.

By defining a quantum-mechanical operator that corresponds to the filtered spin torque, we can obtain a formal expression for the filtered spin noise that does not depend on the power spectrum of the fluctuations. As discussed in Appendix A 1, our sensitivity analysis assumes that the signal torque is analyzed by means of a matched filter L, chosen in such a way that the value being measured appears at the filter output. The operator corresponding to the experimental observable can thus be defined as the filter output T_L in response to the operator input $T(t)$. If instrument noise is negligible, quantum-statistical uncertainty in T_L is the only source of shot-to-shot variation in the measurement. Noise associated with spin fluctuations can therefore be identified with this uncertainty. In particular, the variance in the measured value due to filtered spin noise is

$$\sigma_{\text{spin}}^2 = \langle T_L^2\rangle - \langle T_L\rangle^2. \tag{11}$$

The filter L is defined in Appendix A 1 by Eqs. (A3), (A7), and (A8), and T_L is given by Eq. (A18). With proportionality constants suppressed, we have

$$T_L \propto \int_{t_1}^{\infty} I_x(t)\,\langle I_x(t)\rangle\; dt,$$

where the lower limit of integration corresponds to the beginning of the detection period. From Eq. (A22),

$$\sigma_{\text{spin}}^2 \propto \int_{t_1}^{\infty}\int_{t_1}^{\infty} [\langle I_x(t)I_x(t')\rangle - \langle I_x(t)\rangle\langle I_x(t')\rangle] \times \langle I_x(t)\rangle\langle I_x(t')\rangle\, dt'\, dt,$$

which shows that σ_{spin}^2 can be interpreted as the output of a two-dimensional filter, where the spin fluctuations characterized by

$$\langle I_x(t)I_x(t')\rangle - \langle I_x(t)\rangle\langle I_x(t')\rangle$$

are the filter input.

In Appendix B, we evaluate σ_{spin}^2 for the example where a single spin is detected by a resonator at 0 K during free precession, and we show that for detection of N spins during ideal pulsed spin locking, σ_{spin}^2 depends on the details of the internal spin Hamiltonian H_{int}. For the sensitivity analysis presented here, a rough estimate of the filtered spin noise in an N-spin system is sufficient. Rather than doing a detailed study of the dependence of σ_{spin}^2 on H_{int}, we use a simple model of the spin fluctuations to make this estimate.

In developing the model, we identify the unfiltered fluctuations in the spin torque with uncertainty in the operator $T(t)$. The mean-square fluctuation is given by

$$\langle T^2(t)\rangle - \langle T(t)\rangle^2 = \left[\gamma\hbar\frac{dB_x}{d\theta}\Delta I_x(t)\right]^2, \tag{12}$$

where $[\Delta I_x(t)]^2$ denotes the variance in $I_x(t)$. Since most of our attention is focused on the case where instrument noise is the dominant noise source, our estimate of the spin noise is used to characterize the conditions under which it can be neglected. We therefore wish to replace the time-dependent term $\Delta I_x(t)$ by a constant term that functions as a rough upper bound. Note that for a system of N spins 1/2 in thermal equilibrium, the uncertainty of all spin components is maximized when $P \approx 0$, since

$$(\Delta I_z)^2 = \frac{N}{4}(1 - P^2)$$

and

$$(\Delta I_x)^2 = (\Delta I_y)^2 = \frac{N}{4}.$$

Our model of spin noise replaces $[\Delta I_x(t)]^2$ in Eq. (12) by $N/4$. The spin fluctuations of an unpolarized sample are thus considered to be superimposed on the signal.

We assume that the fluctuations in the spin-locked component decay exponentially with time constant $T_{1\rho}$, while the fluctuations in the other components decay so quickly that their contribution to the filtered spin noise can be neglected. In the laboratory frame, slow fluctuations in the spin-locked component cause variation in the amplitude of the oscillating spin torque. We treat the amplitude fluctuations as a stationary random process, described by the correlation function

$$C_{\text{spin}}(t,t') = \frac{N}{4}\left(\gamma\hbar\frac{dB_x}{d\theta}\right)^2 e^{-|t'-t|/T_{1\rho}}$$

and the single-sided spectral density

$$S_{\text{spin}}(\omega) = N\left(\gamma\hbar\frac{dB_x}{d\theta}\right)^2 \frac{T_{1\rho}}{1+\omega^2 T_{1\rho}^2}. \tag{13}$$

The variance of the spin noise appearing at the filter output is then given by Eq. (A17) as

$$\sigma_{\text{spin}}^2 = \frac{N}{2}\left(\gamma\hbar\frac{dB_x}{d\theta}\right)^2. \tag{14}$$

4. Signal-to-noise ratio

The signal-processing scheme described in Appendix A 1 is designed to yield an estimate of

$$s(t_1) = \gamma\hbar \frac{dB_x}{d\theta} \langle I_x(t_1)\rangle ,$$

where $s(t)$ is the signal defined by Eq. (5) and where time t_1 corresponds to the beginning of the detection period. The variance of the measured value is

$$\sigma^2 = \sigma_{\text{inst}}^2 + \sigma_{\text{spin}}^2,$$

where σ_{inst}^2 and σ_{spin}^2 are given by Eqs. (10) and (14), respectively. Defining the single-shot SNR ρ by

$$\rho = \frac{|s(t_1)|}{\sigma},$$

we obtain

$$\rho = \frac{|\gamma\hbar\,(dB_x/d\theta)\,\langle I_x(t_1)\rangle|}{\sqrt{(2/DT_{1\rho})S_{\text{inst}} + (N/2)\,[\gamma\hbar\,(dB_x/d\theta)]^2}}. \tag{15}$$

Note that Eq. (15) gives ρ as a function of t_1, since the numerator depends on t_1. The single-shot SNR for the experiment is found by averaging $\rho^2(t_1)$ over the sampled values of t_1 and then taking the square root.

Much of our attention is focused on the case where instrument noise is the dominant noise source, with $\langle I_x(t_1)\rangle = PN/2$, and with the effect of the duty cycle D neglected. Under these conditions, we have

$$\rho = PN\frac{(\gamma\hbar/2)(dB_x/d\theta)}{\sqrt{(2/T_{1\rho})S_{\text{inst}}}}. \tag{16}$$

In Eq. (16) and in similar equations appearing later in the paper, the absolute value sign has been dropped from the numerator to simplify notation.

B. Detection of spin-noise correlations

In order to characterize the sensitivity enhancement associated with sample polarization, we analyze the sensitivity of the CONQUEST detection scheme, which encodes spectra into measurements of spin-noise correlations and thus does not require sample polarization. Only a brief description of the scheme is presented here; additional details can be found in Refs. 20 and 21. We consider the regime where the resonator temperature is low, as required for sensitive detection, but where spin relaxation to thermal equilibrium between transients is inconveniently slow. The sample is thus assumed to be unpolarized.

Although the mean value of the sample dipole is zero, the instantaneous dipole moment is in general nonzero due to imperfect cancellation of the randomly-oriented spins.[38] Note that a nonzero dipole moment can be identified with spin noise, since it represents a fluctuation away from the mean. In the CONQUEST scheme, the dipole of the fluctuating spin system is measured both before and after a period of coherent evolution under a Hamiltonian H that is of spectroscopic interest. In the case where the transverse spin component I_x is detected, the two measurements yield an estimate of the correlation function $\langle I_x(t_1)I_x\rangle$, where $t = 0$ and $t = t_1$ are the times of the first and second measurement, respectively.[20] A record of the evolution under H is obtained by varying the evolution time t_1.

In comparing the sensitivity of BOOMERANG and CONQUEST, we refer to the respective schemes as "first-order" and "second-order" methods, highlighting the fact that the signals are proportional to $\langle I_x(t_1)\rangle$ and $\langle I_x(t_1)I_x\rangle$. Note that the strategy behind the second-order method is to use an initial measurement to increase our knowledge of the sample dipole. We can therefore expect it to be more sensitive than the first-order method in the regime where the mean dipole is small compared to the fluctuations and where instrument noise is negligible. The sensitivity of the two methods in this regime has been analyzed.[20] Under the simplifying assumption that the evolution of the Heisenberg operator $I_x(t)$ under H is given by

$$I_x(t_1) = I_x\cos(\omega t_1) + I_y\sin(\omega t_1), \tag{17}$$

the SNR of the second-order method is

$$\rho_2 = \frac{\sqrt{N}\cos(\omega t_1)}{\sqrt{N + (N-2)\cos^2(\omega t_1)}}. \tag{18}$$

Equation (18) takes account of the shot-to-shot variation associated with quantum-mechanical uncertainty in the operator $\langle I_x(t_1)I_x\rangle$. Weak polarization is assumed, with $P\sqrt{N} \ll 1$. For $\cos(\omega t_1) = 1$, we obtain

$$\rho_2 = \frac{1}{\sqrt{2 - 2/N}} \sim 1.$$

By way of contrast, the sensitivity of the first-order method in the same regime is

$$\rho_1 = P\sqrt{N} \ll 1.$$

Equation (18) was obtained by using projection operators to represent the measurement process. To characterize sensitivity in the regime where instrument noise is non-negligible, we use a model of the experiment in which the period of evolution under H is sandwiched between two detection periods of ideal pulsed spin locking. As in the analysis of Sec. II A, the resonator is assumed to be continuously observed throughout the experiment, and the measured coordinate $\theta_{\text{obs}}(t)$ is converted to a torque $T_{\text{obs}}(t)$. For the sensitivity analysis, we can consider the acquired data to consist of the two-dimensional function

$$y(t,t') = T_{\text{obs}}(t)T_{\text{obs}}(t'). \tag{19}$$

The noiseless signal is

$$s(t,t') = \langle T(t)T(t')\rangle = \left(\gamma\hbar\frac{dB_x}{d\theta}\right)^2 \langle I_x(t)I_x(t')\rangle,$$

and the signal-processing protocol yields an estimate of

$$s(t_1,0) = \left(\gamma\hbar\frac{dB_x}{d\theta}\right)^2 \langle I_x(t_1)I_x\rangle. \tag{20}$$

The measured torque $T_{\text{obs}}(t)$ includes instrument noise $N_{\text{inst}}(t)$ associated with resonator fluctuations and detection of the mechanical motion. As shown in Sec. III C, instrument noise in the measurement bandwidth is expected to be larger than spin noise for sufficiently small samples. In particular, the torque due to instrument noise in a bandwidth $\Delta\nu \sim 1/T_{1\rho}$ is larger than the torque from an unpolarized sample containing

up to a few tens of nuclei, even if instrument noise is reduced to a level near the quantum-mechanical limit. We therefore make the simplifying assumption that the noise in $y(t,t')$ is dominated by the product $N_{\rm inst}(t)N_{\rm inst}(t')$. In the regime defined by this assumption, the sensitivity advantage associated with measuring spin-noise correlations is limited by the need to make two measurements per transient using a noisy detector.

The sensitivity of the second-order scheme in this regime can be quantified by an analysis based on the signal-processing protocol described in Appendix A 2. The signal is expressed in the form $s(t,t') = Gs_0(t,t')$, where s_0 is a known function, and where $G = s(t_1,0)$ is given by Eq. (20). An estimate of G is obtained from the noisy data using a two-dimensional filter, defined by Eqs. (A25) and (A26). Appendix C carries out the sensitivity analysis in the case where the evolution of $I_x(t)$ under H is described by Eq. (17). The SNR is found to be

$$\rho_2 = N\frac{(\gamma\hbar/2)^2\,(dB_x/d\theta)^2}{(2/T_{1\rho})S_{\rm inst}}, \tag{21}$$

where $\cos(\omega t_1)$ has been set to 1.

Since the second-order method involves a product of two noisy measurements, ρ_2 is closely related to ρ_1^2, where ρ_1 represents the SNR for the first-order method in the regime where spin noise is small compared to instrument noise. Indeed, we find from Eq. (16) that

$$\rho_1^2 = (PN)^2\,\frac{(\gamma\hbar/2)^2(dB_x/d\theta)^2}{(2/T_{1\rho})S_{\rm inst}}. \tag{22}$$

The difference in the dependence of Eqs. (21) and (22) on P and N is due to the fact that $\langle I_x^2\rangle \sim N$ in an unpolarized sample, while $\langle I_x\rangle^2 \sim (PN)^2$ in a polarized sample.

C. Comparison of the detection sensitivities

For samples sufficiently small that instrument noise is the dominant source of variance in the measurement, Eqs. (21) and (22) imply that

$$\rho_1 = \left(\frac{P^2N}{\rho_1}\right)\rho_2. \tag{23}$$

The relative sensitivity of the methods is thus given by the ratio P^2N/ρ_1. When $P^2N > \rho_1$, we gain more information about the initial spin dipole by letting the sample relax to thermal equilibrium than by using the noisy detector to measure a spin fluctuation.

An alternative way to make the comparison is to note that the first-order method is more sensitive when

$$P > \frac{\rho_1}{PN}.$$

Sample polarization thus improves sensitivity when P is larger than the SNR for detection of a fully-polarized spin in a single transient.

Even if instrument noise is reduced to a level near the quantum-mechanical limit, the "sensitivity per polarized spin" ρ_1/PN is substantially less than 1. In Sec. III C, a numerical example is used to characterize sensitivity in this regime. Under the assumption of ideal spin locking, the parameters $\omega_h/2\pi = 600$ MHz, $T_h = 10$ mK, and $A = 16$ yield $P = 0.9$ and $\rho_1/PN = 0.08$. For this example, detection of the polarized sample dipole would be more sensitive than detection of spin-noise correlations by an order of magnitude. Under conditions where instrument noise is significantly larger than this near-optimal level, resonator-induced polarization of order unity would yield larger sensitivity enhancements.

It should be pointed out that Eq. (23) compares single-shot sensitivities rather than acquisition times. Unlike the first-order method, the second-order method does not require a period of sample polarization between transients.[20] A more thorough comparison of the two methods would need to take account of the time constants that limit the repetition rate in a given experimental context. Equation (23) is useful as a simple characterization of the conditions where sample polarization improves single-shot sensitivity.

III. RESONATOR-INDUCED SIGNAL DECAY

A. Signal lifetime

For the detection scheme described in Sec. II A 1, pulsed spin locking optimizes the signal energy by collapsing the detected transient into a narrow bandwidth and counteracting resonator-induced signal decay due to dissipation[23] and radiation damping. Since pulsed spin locking is a well-established tool for averaging the internal spin Hamiltonian to obtain a narrow signal bandwidth,[27–32] the discussion here is limited to the problem of slowing resonator-induced signal decay.

During a period of pulsed spin locking, the rotating-frame Hamiltonian for the rf field can be expressed in the form $H_{\rm rf} = \omega_1(t)I_x$, where the time-dependence of $\omega_1(t)$ is due to the cyclical pulsing of the field. It is convenient to express $\omega_1(t)$ as

$$\omega_1(t) = \bar{\omega}_1 + \omega_p(t),$$

where $\bar{\omega}_1$ is the average of $\omega_1(t)$ over one cycle.[27] A strong time-averaged component $\bar{\omega}_1$ functions as a spin-locking field, and the sidebands associated with the periodic term $\omega_p(t)$ do not hinder the averaging process, provided the spacing between pulses is sufficiently short.[27] The spacing between pulses can be characterized by the nutation angle per cycle

$$\phi_p = \bar{\omega}_1\tau_p,$$

where τ_p is the period of the modulation cycle. While initial investigations of pulsed spin locking focused on the case where $\phi_p = \pi/2$,[27] other values of ϕ_p have also been used.[28,30–32]

The approach previously used to analyze resonator-induced relaxation during continuous spin locking[23] can be adapted to the study of pulsed spin locking. We limit the discussion to the case where the bandwidth of the mechanical fluctuations is broad compared to the maximum value of $|\omega_1(t)|$, as well as to the spectral width of $H_{\rm int}$. The spins are assumed to have identical couplings to the resonator. The rotating-frame master equation governing the evolution of the spin density matrix σ is[14,25]

$$\frac{d\sigma}{dt} = -i\,[H_{\rm int} + H_{\rm rf},\sigma] + \Lambda\sigma. \tag{24}$$

In Eq. (24), Λ is a relaxation superoperator, given by

$$\begin{aligned}\Lambda\sigma \;=\; & R_0\,(n_{\rm th}+1)\left(I_+\sigma I_- - \tfrac{1}{2}[I_-I_+,\sigma]_+\right)\\ & + R_0 n_{\rm th}\left(I_-\sigma I_+ - \tfrac{1}{2}\,[I_+I_-,\sigma]_+\right),\end{aligned} \tag{25}$$

where R_0 is the rate constant governing spontaneous emission by the spins into the resonant mode,[14] and where I_+ and I_- are the raising operator and lowering operator, respectively, summed over the spins. For reference later in the discussion, we note that[14]

$$R_0 = 2g^2\tau_h, \tag{26}$$

where

$$g = \frac{-\gamma}{2}\sqrt{\frac{\hbar}{2I_h\omega_h}}\frac{dB_x}{d\theta} \tag{27}$$

is the coupling constant for the resonant interaction between the spins and the mechanical oscillator, which is governed by the Hamiltonian

$$H_1 = g(I_+a^\dagger + I_-a). \tag{28}$$

In Eq. (28), $a^\dagger$ and a are the raising and lowering operators for the harmonic oscillator, respectively. The product operators appearing in H_1 exchange a quantum of energy between the spins and the resonator; this resonant exchange survives averaging over the fast unperturbed motion of the spins and the oscillator. Equations (25) and (28) assume $\gamma > 0$ and incorporate the convention that the time-averaged field at the spins points along the positive z axis. If the sign of γ is reversed, resonant exchange of quanta is governed by the operators $I_-a^\dagger$ and I_+a, as in the conventional description of the coupling between two-level atoms and a cavity mode of the electromagnetic field.[24] Consistent with Eqs. (25) and (28), we assume throughout Sec. III that $\gamma > 0$.

Letting $U_{\rm rf}$ represent the propagator associated with the applied rf field, we transform Eq. (24) to the reference frame where $H_{\rm rf}$ has been eliminated, commonly known as the toggling frame:

$$\frac{d\tilde{\sigma}}{dt} = -i[\tilde{H}_{\rm int},\tilde{\sigma}] + \tilde{\Lambda}\tilde{\sigma}. \tag{29}$$

In Eq. (29), a tilde over an operator A indicates the transformation of A into the toggling frame,

$$\tilde{A} = U_{\rm rf}^{-1}AU_{\rm rf}, \tag{30}$$

and $\tilde{\Lambda}\tilde{\sigma}$ is obtained by transforming each operator on the right side of Eq. (25) into the toggling frame.

Transformation into the toggling frame causes the internal Hamiltonian and the relaxation superoperator to become time dependent. If the flip angle ϕ_p satisfies the equation $n\phi_p = m2\pi$, where n, m are integers, then $\tilde{H}_{\rm int}$ and $\tilde{\Lambda}$ oscillate periodically in time $T_p = n\tau_p$.[39] For simplicity, we assume that $m = 1$, so that $T_p = 2\pi/\bar{\omega}_1$.

Consider first the case where $H_{\rm int} = 0$ and where T_p is sufficiently short that $\tilde{\Lambda}$ can be approximated by its time average, which we denote by Λ_1. Appendix D shows that Λ_1 is given by

$$\begin{aligned}\Lambda_1\tilde{\sigma} = {} & R_h\left(I_x\tilde{\sigma}\,I_x - \tfrac{1}{2}\left[I_x^2,\tilde{\sigma}\right]_+\right) + a^2R_h\left(I_y\tilde{\sigma}\,I_y - \tfrac{1}{2}\left[I_y^2,\tilde{\sigma}\right]_+\right)\\ & + b^2R_h\left(I_z\tilde{\sigma}\,I_z - \tfrac{1}{2}\left[I_z^2,\tilde{\sigma}\right]_+\right).\end{aligned} \tag{31}$$

In Eq. (31), a^2 and b^2 are numbers that depend on the details of the modulation cycle and satisfy $a^2 + b^2 = 1$, and

$$R_h = R_0\,(2n_{\rm th} + 1) \tag{32}$$

is the rate constant governing resonator-induced polarization.[14] As in the case of continuous spin locking, averaging of Λ by the spin-locking field yields a superoperator that can be interpreted as relaxing individual spins independently.[23] The resulting equation of motion for the spin-locked component $\langle I_x\rangle$ is

$$\frac{d}{dt}\langle I_x\rangle = -\frac{R_h}{2}\langle I_x\rangle, \tag{33}$$

which gives

$$T_{1\rho} = 2/R_h. \tag{34}$$

In the general case, $\tilde{\Lambda}$ can be replaced with its average only if the modulated terms in $\tilde{\Lambda}$ oscillate quickly on the time scale of the evolution governed by Eq. (29). Physically, the resonator-induced transitions responsible for signal decay are averaged only if the entire spin system nutates about the spin-locking field, which requires the averaging of $\tilde{H}_{\rm int}$ as well as $\tilde{\Lambda}$. If $\bar{\omega}_1$ is sufficiently large, and if ϕ_p is chosen so as to eliminate slowly-oscillating secular terms from $\tilde{H}_{\rm int}$,[27] then $\tilde{H}_{\rm int}$ and $\tilde{\Lambda}$ can both be approximated by their time averages in Eq. (29). The toggling-frame master equation simplifies to

$$\frac{d\tilde{\sigma}}{dt} = -i[\bar{H}_{\rm int},\tilde{\sigma}] + \Lambda_1\tilde{\sigma}, \tag{35}$$

where $\bar{H}_{\rm int}$ represents the time average of $\tilde{H}_{\rm int}$. Note that $\phi_p = \pi/2$ guarantees both that $\tilde{H}_{\rm int}$ does not contain slowly-oscillating secular terms and that $\bar{H}_{\rm int}$ commutes with I_x.[27] The commutator in Eq. (35) then makes no contribution to the evolution of $\langle I_x\rangle$, and we recover Eqs. (33) and (34).

Although evolution under $H_{\rm int}$ would typically be expected to occur on a shorter time scale than the transitions associated with the relaxation superoperator, it is possible that when many spins are present and the coupling to the resonator is strong, radiation damping could determine the time scale for the evolution of $\tilde{\sigma}$ and thus the necessary strength of the spin-locking field. To find the characteristic time for radiation damping, we use a macroscopic model presented by Abragam,[40] in which a precessing sample dipole $\boldsymbol{\mu}$ nutates toward alignment with the static field due to the backaction of the resonator. Abragam's derivation for an inductive resonator can easily be adapted to a mechanical resonator, and we find that the nutation of $\boldsymbol{\mu}$ is described by the equation

$$\frac{d\alpha}{dt} = -R_0\,(\mu/\gamma\hbar)\sin\alpha, \tag{36}$$

where α represents the angle between $\boldsymbol{\mu}$ and the static field. For a system of spins 1/2, radiation damping is thus roughly characterized by the angular frequency

$$\omega_{\rm rd} = R_0\,(PN/2),$$

the maximum angular derivative obtained from Eq. (36) by identifying μ with $\gamma\hbar PN/2$. In discussing resonator design in Sec. IV C, we use $\omega_{\rm rd}$ as a measure of the coupling between the sample and the resonator, illustrating the way in which it depends on parameters of the spin-resonator system.

We simulated resonator-induced signal decay in three-spin and four-spin systems in order to characterize the effectiveness of nonideal pulsed spin-locking in extending signal lifetime. Twenty structures that contained carbon, nitrogen, oxygen, and either three or four hydrogen atoms were randomly selected from the Cambridge Structural Database (CSD).[41] Resonator-induced signal decay during continuous spin-locking with $\omega_1/2\pi = 50$ kHz was previously simulated for these systems.[23] Since some systems included dipolar couplings in the range of 25–30 kHz, departures from ideality were observed. We used the methods described in Ref. 23 to simulate resonator-induced signal decay in the same systems during pulsed spin locking with $\bar{\omega}_1/2\pi = 50$ kHz and $\phi_p = \pi/2$. The decay curves were nearly identical to those for continuous spin locking with $\omega_1/2\pi = 50$ kHz, independent of the pulse width.

B. Sensitivity limit

The sensitivity formula for detection of a polarized sample dipole can be significantly simplified when $T_{1\rho} = 2/R_h$ and $D = 1$. Equations (26), (27), and (32) can be used to obtain an explicit formula for $T_{1\rho}$, and substitution of this formula into Eq. (15) yields

$$\rho = \frac{|\langle I_x(t_1)\rangle|}{\sqrt{(2n_{\rm th}+1)(2n_{\rm th}+1+2A)+N/2}}. \tag{37}$$

In the case where spin noise is negligible compared to instrument noise and $\langle I_x(t_1)\rangle = PN/2$, Eq. (37) reduces to

$$\rho = \frac{PN/2}{\sqrt{(2n_{\rm th}+1)(2n_{\rm th}+1+2A)}}. \tag{38}$$

The factor $(2n_{\rm th}+1)$ under the radical can be traced to Eq. (32), where it characterizes the extent to which thermally-stimulated spin transitions contribute to resonator-induced relaxation. If this factor is set to 1, the relaxation is due entirely to spontaneous emission, which is governed by the rate constant R_0. The factor $(2n_{\rm th}+1+2A)$ comes from Eq. (9), which gives the spectral density of the instrument noise.

Note that P and $n_{\rm th}$ depend on the properties of the spin-resonator system only through the parameter ω_h/T_h. Equation (38) thus implies that if γ, τ_h, I_h, and $dB_x/d\theta$ were "knobs" that could be controlled experimentally, the single-shot SNR per spin would be unaffected as these knobs were turned, provided ω_h/T_h and A were held constant. Changes in the signal lifetime would exactly compensate for changes in the coupling strength and the noise power.

Note as well that the criterion for a classical description of the resonator to be valid is $\omega_h/T_h \ll k_B/\hbar$. Near-optimal sensitivity corresponds to the regime where departures from classical behavior are significant, with $P \sim 1$ and $n_{\rm th} < 1$, and ideal measurement conditions are approached asymptotically as the temperature is lowered. For a fixed value of A in Eq. (38), we can roughly say that the sensitivity per spin depends only on "how quantum mechanical" the resonator is.

The cancellation of parameters from Eq. (38) is due to the presence of the following three terms: (1) the factor $\gamma(dB_x/d\theta)$ in the signal torque, (2) the factor $\omega_h I_h/\tau_h$ in the spectral density of the instrument noise, and (3) the factor $1/R_0$ in the signal lifetime. In general, the same three terms are present if the noise power is associated with resonator fluctuations and if the signal lifetime is limited by decay due to resonator-induced spin transitions. Rather than being an artifact of the detection scheme or the assumption of ideal spin locking, the cancellation of the parameters associated with these terms is due to a balance between three physical quantities, and it can be considered a fundamental aspect of resonant signal detection in the low-temperature regime.

Consider, for example, the way in which sensitivity is affected by the duty cycle of the detection during pulsed spin locking. Dropping the simplifying assumption that $D = 1$ causes the right side of Eq. (38) to be multiplied by $\sqrt{D}$. The decay time τ_h then influences sensitivity indirectly, since it affects the duty cycle. However, a balance between the coupling strength, the noise power, and the signal lifetime still exists: If the parameters of the spin-resonator system are varied, with ω_h/T_h held constant, the combined effect of the changes in these three quantities leaves sensitivity unchanged. The same balance exists for the detection of spin-noise correlations, as characterized by Eq. (21).

More generally, consider the case where the detailed functional form of a filtered spin signal is characterized by means of a set of sampled points. Direct detection of an FID would typically correspond to this case, for example. As discussed in connection with Eq. (A24), the SNR can be defined by

$$\rho^2 = \sum_k \frac{s_L^2(t_k)}{\langle n_L^2\rangle},$$

where s_L and n_L are the filtered signal and noise, respectively, and where t_k ranges over the set of sampled points. We can consider this sum to be proportional to the signal energy E. Since Eq. (25) implies that the time scale of resonator-induced decay is $\propto 1/R_0$, we have $E \propto 1/R_0$ if the resonator is the dominant source of signal decay, which gives $\rho \propto \sqrt{E} \propto 1/\sqrt{R_0}$. If the resonator is also the dominant noise source, then parameters associated with the coupling strength, the noise power, and the signal lifetime cancel from the sensitivity formula, which implies a balance between these three quantities.

This cancellation of parameters can be generalized beyond force-detected magnetic resonance. Formally, the spin-resonator system under consideration consists of a damped harmonic oscillator weakly coupled to spins by the Hamiltonian H_1 of Eq. (28). An additional formal feature of the system is that the evolution governed by H_1 is slow on the time scale of the oscillator's relaxation to thermal equilibrium, which implies that quanta transferred from the spins to the oscillator are quickly dissipated into the thermal bath, rather than being cycled back to the spins. Under these conditions, the oscillator perturbs the spin evolution only by causing signal decay through the action of the relaxation superoperator Λ,[14,25] given by Eq. (25). For a detector described formally as a damped harmonic oscillator weakly coupled to spins by the resonant interaction H_1, the detection sensitivity can be analyzed using arguments similar to those we have presented for the torsional resonator.[42] Physical examples include Rydberg

atoms coupled to a damped cavity mode[25] and nuclear spins coupled to a tuned circuit[14] or a mechanical resonator. The balance between the coupling strength, the noise power, and the signal lifetime can be generalized to the case where this formal description of the system is applicable and where the detector is both the dominant noise source and the dominant source of signal decay.

The balance between these quantities is associated with an intrinsic sensitivity limit for resonant detection of coherent spin evolution. In characterizing this limit, we consider an example where a freely precessing spin 1/2 is detected by a resonator at 0 K, and where the noise added during the transduction and amplification of the resonator signal is quantum limited. The spin is aligned with the x axis at the beginning of the detection period, and the decay of the spin signal is due to spontaneous emission into the resonator. The resulting time constant for transverse relaxation is $T_2 = 2/R_0$.[23] We assume that a matched filter is used to extract the signal from the noise, with the output of the filter an estimate of the signal torque at the beginning of the detection period,

$$s(0) = \frac{1}{2}\gamma\hbar\frac{dB_x}{d\theta}.$$

The filter bandwidth is given by Eq. (A23) as

$$\Delta\nu = 2/T_2 = R_0,$$

and the variance in the measurement due to instrument noise is

$$\sigma^2_{\text{inst}} = S_{\text{inst}}\Delta\nu = 2\left(\gamma\hbar\frac{dB_x}{d\theta}\right)^2,$$

where the spectral density S_{inst} of Eq. (9) is evaluated at the mechanical frequency, with $n_{\text{th}} = 0$ and $A = 1/2$. As discussed in Sec. II A3, filtered spin noise can be identified with quantum-statistical uncertainty in the operator that corresponds to the filtered spin torque. The variance σ^2_{spin} due to spin noise is given by Eq. (B6) as

$$\sigma^2_{\text{spin}} = \frac{1}{4}\left(\gamma\hbar\frac{dB_x}{d\theta}\right)^2.$$

The quantum-limited SNR for resonant detection of a spin signal is therefore

$$\frac{|s(0)|}{\sqrt{\sigma^2_{\text{inst}} + \sigma^2_{\text{spin}}}} = \frac{1}{3}.$$

C. Near-optimal sensitivity

Section II C compares the sensitivities of two spectroscopic detection schemes in the regime where instrument noise is the dominant noise source. The condition for sample polarization to improve sensitivity is $P > \rho/PN$, where ρ/PN is the sensitivity for detection of a fully-polarized spin during a single transient.

Equation (38) can be used to characterize ρ/PN under near-optimal measurement conditions. We assume ideal spin locking with duty cycle $D = 1$, and near-ideal motion detection with noise number $A = 16$, which has been achieved at millikelvin temperatures using a single-electron transistor.[43] Frequency $\omega_h/2\pi = 600$ MHz and temperature $T_h = 10$ mK give $n_{\text{th}} = 0.06$ and $P = 0.9$, which are close to the limiting values. From Eq. (38), we then obtain $\rho/N = 0.07$ and $\rho/PN = 0.08$.

The relative magnitude of spin noise and instrument noise under these measurement conditions can be roughly estimated by means of Eq. (37). Spin noise is smaller than instrument noise when

$$N/2 < (2n_{\text{th}} + 1)(2n_{\text{th}} + 1 + 2A),$$

which corresponds to $N \lesssim 75$. Note that this estimate is based on a model of spin noise in which the fluctuations of an unpolarized sample are superimposed on the polarized spin dipole, as discussed in Sec. II A3. This simple model was chosen to overestimate the spin noise, and it is likely that a more accurate model would give a larger estimate of the number of spins needed for spin noise and instrument noise to be equal.

IV. RESONATOR DESIGN

A. Acquisition time

Although the single-shot sensitivity per spin of Eq. (38) is independent of most resonator parameters, the rate constant R_h that governs resonator-induced polarization between transients depends strongly on resonator parameters. The number of transients required to detect a spectrum with acceptable sensitivity is $\propto 1/\rho^2$, and if the time per transient is $\propto 1/R_h$, then the acquisition time is $\propto 1/R_h\rho^2$. In minimizing the acquisition time, we thus maximize

$$R_h\rho^2 \propto \tau_h\left(\frac{dB_x/d\theta}{\sqrt{I_h}}\right)^2\frac{P^2}{\omega_h(2n_{\text{th}} + 1 + 2A)}, \tag{39}$$

where the spin noise and the duty cycle have been neglected. The dependence on $(dB_x/d\theta)/\sqrt{I_h}$ is due to the presence of this factor in Eq. (27), which gives the coupling constant g for the resonant interaction that exchanges quanta between the spins and the harmonic oscillator. The dependence on τ_h arises because the resonator's correlation time limits the period during which spin-resonator correlations can build up before being disrupted by fluctuations. Since the magnitude of these correlations determines the rate at which quanta are exchanged, $R_h \propto \tau_h$.

The optimal frequency for fast acquisition depends on the function

$$f(\omega) = \frac{P^2(\omega)}{\omega[2n_{\text{th}}(\omega) + 1 + 2A]}. \tag{40}$$

In Eq. (40), the denominator contains a factor of ω because $R_h \propto 1/\omega_h$, while the remaining terms can be traced to the SNR formula of Eq. (38). The values of T_h and A determine the frequency at which f reaches its maximum. For quantum-limited detection at $T_h = 10$ mK, the optimum is $\omega_h/2\pi \approx 525$ MHz, and the value of f stays within 10% of its peak value over the range 375 to 775 MHz. Increasing A by a factor of 20 shifts this range slightly, so that f stays within 10% of its peak value from 300 to 700 MHz.

From examination of Eq. (39), we see that an optimal resonator will be weakly damped and have both a strong

angular field derivative at the spins and a small moment of inertia. A similar set of criteria has been obtained for MRFM cantilevers,[3] where the angular field derivative and moment of inertia are replaced by the field gradient and motional mass, respectively. Note that if the signal lifetime $T_{1\rho}$ is not limited by resonator-induced decay, but is instead shortened by dephasing of the transverse dipole under $H_{\rm int}$ or by imperfections in the pulsed rf field, the same three criteria are significant for optimization of either the sensitivity or the acquisition time. From Eq. (16), for example, we obtain

$$\rho^2 \propto T_{1\rho}\,\tau_h \left(\frac{dB_x/d\theta}{\sqrt{I_h}}\right)^2 \frac{P^2}{\omega_h\,(2n_{\rm th}+1+2A)}. \qquad (41)$$

For a torsional resonator coupled to spins by a torque of the form $\gamma\hbar\,(dB_x/d\theta)\,I_x$, the sample can in principle be placed arbitrarily close to the magnets without increasing the friction that damps the resonator.[15] Damping due to relative motion between the sample and nearby moving magnets, which has limited the sensitivity of MRFM,[1] is associated with the use of translational oscillators as detectors. A spin-resonator coupling is present only if the mechanical oscillations modulate the field at the spins; in the case where the oscillations cause magnets to move along a straight line, there is no coupling if the spin sample moves in unison with the magnets. However, rotation of the sample and the magnets in unison allows for the presence of a torque proportional to $dB_x/d\theta$. Note as well that the torque does not depend on a field gradient; it exists even if the resonator's field at the spins is perfectly homogeneous. This form of spin-resonator coupling is advantageous for spin polarization. Placing the spins arbitrarily close to the magnets gives a maximal value of $dB_x/d\theta$ and allows for a small motional mass. The lack of dependence on a gradient facilitates the optimization of field homogeneity, needed for the efficient polarization of samples containing many spins and for the resolution of spectroscopic splittings.

B. Coupling strength

Whether the single-shot sensitivity or the acquisition time is used as a figure of merit, optimal performance depends on the presence of a large applied field B_0. Even with a temperature as low as $T_h = 10$ mK, for instance, an applied field of order 10 T is needed for near-optimal detection of H nuclei with $P \sim 1$. A field of this magnitude will tend to saturate the resonator's magnetization $\mathbf{M}$ and hold it pinned along the direction of the field during the mechanical oscillations. This effect is illustrated in Fig. 2(a), which shows two limiting cases for the orientation of $\mathbf{M}$ after the resonator of Fig. 1 has rotated away from the equilibrium position. The limiting case where $\mathbf{M}$ rotates with the cylinders is incompatible with the presence of an applied field sufficiently large to yield $P \sim 1$.

Indeed, the opposite limiting case, where $\mathbf{M}$ remains aligned with the applied field, can be considered a good description of the resonator's magnetization unless the magnets are fabricated from a material with a large crystal anisotropy. Calculation of R_h for simple resonator designs showed that polarization times ∼1 s can occur when magnet dimensions are ∼100 nm. Since magnetic particles in this size range often consist of a single magnetic domain,[44] and since an applied field ∼10 T would be substantially larger than the demagnetizing field, $\mathbf{M}$ can be modeled as uniform when the resonator is in the equilibrium position. To characterize the error associated with the approximation that $\mathbf{M}$ remains continually aligned with the applied field field during the mechanical oscillations, we used a model in which the resonator's cylindrical magnets were replaced by uniformly-magnetized spheroids. Formulas for the demagnetizing fields within the spheroids[45] were used to find the minimum-energy orientation of $\mathbf{M}$ corresponding to a given angular displacement of the resonator. For this model, the angular displacement of $\mathbf{M}$ is only a few percent of the resonator's displacement θ for $M \sim 2\ \mathrm{T}/\mu_0$ and $B_0 \sim 10$ T, with the effects of crystal anisotropy neglected.[46]

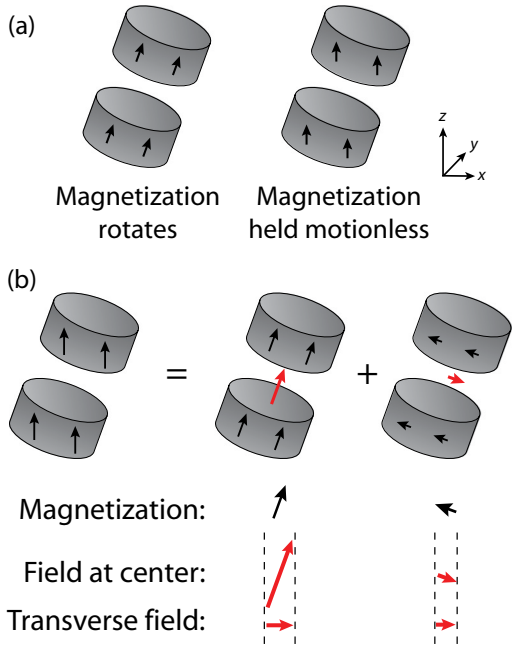

FIG. 2. (Color online) Comparison of the resonator's transverse field in two limiting cases. In (a), arrows represent the magnetization $\mathbf{M}$ of the resonator's ferromagnetic cylinders after a mechanical rotation away from the equilibrium position. In (b), magnetization that remains aligned with the applied field is expressed as the sum of two perpendicular components, one of which rotates with the cylinders. The transverse fields generated by the two components add constructively at the location of the spins. If $\mathbf{M}$ rotates with the cylinders, only the first of these components is present. The spin-resonator coupling is thus stronger when $\mathbf{M}$ remains aligned with the applied field during the mechanical oscillations.

Interestingly, the spin-resonator coupling is optimal in the case where $\mathbf{M}$ is held motionless by the applied field. Figure 2(b) presents a qualitative explanation of this result. Magnetization that remains aligned with the applied field can be expressed as the sum of two perpendicular components, one of which rotates with the cylinders. The field generated by each component can be very roughly characterized by replacing the four cylinders on the right side of Fig. 2(b) by dipoles aligned with the magnetization components. This rough model is sufficient to show that the transverse fields generated by the two components add constructively at the spins, yielding a larger field than would be generated if $\mathbf{M}$ rotated with the cylinders.

The enhancement to the coupling due to this effect can be calculated analytically for the model where the resonator's cylindrical magnets are replaced by spheroids. Formulas for the external fields of uniformly-magnetized spheroids[47] can be used to show that when **M** remains aligned with the applied field,

$$\frac{dB_x}{d\theta} = \frac{3}{2}B_h, \tag{42}$$

where B_h is the resonator's field at the spins. Since the corresponding result for magnetization that rotates with the cylinders is $dB_x/d\theta = B_h$, the spin-resonator coupling is enhanced by a factor of $3/2$ when **M** is pinned to the applied field. The qualitative explanation of Fig. 2(b) can be formalized by expressing the magnetization of the spheroids as the sum of two perpendicular components, one of which rotates with the spheroids. The contribution to $dB_x/d\theta$ due to this rotating component is B_h, while the contribution due to the perpendicular component is $B_h/2$.

Equation (42) can be generalized to the case where the resonator's magnets are cylindrically symmetric. If one of the magnetic cylinders shown in Fig. 1 is removed and the other is replaced by a coaxial circle of uniformly-magnetized material, Eq. (42) still holds in the case where the magnetization is pinned to the applied field. More generally, the equation holds for a resonator whose magnets can be described as a continuous sum of such circles.

An upper bound on $dB_x/d\theta$ can be obtained from the model where the resonator's magnets are replaced by spheroids. In the limiting case where the spheroids become arbitrarily long and thin, and where the separation between them is negligible, the derivative achieves its maximum value:

$$\frac{dB_x}{d\theta} = 3\mu_0 M. \tag{43}$$

By way of comparison, the field inside a long, uniformly-magnetized cylinder is $\mu_0 M$. The factor of 3 in Eq. (43) can be associated with two effects: the increase in $dB_x/d\theta$ over B_h by a factor of $3/2$ when **M** does not rotate, and the presence of a finite gap between the spheroids. In the limiting case of a negligible gap, the field of each of the spheroids at the spins is $\mu_0 M$, for a net field $B_h = 2\mu_0 M$.

C. Discussion

In this section we highlight the importance of size constraints for resonator design, as well as the need for further development, particularly with regard to detection of the mechanical motion. The relevant experimental regime is characterized by order-of-magnitude estimates based on the resonator design proposed in Ref. 15 and shown in Fig. 1.

We first note that since $(dB_x/d\theta) \sim B_h$, the parameter $(dB_x/d\theta)/\sqrt{I_h}$ appearing in Eqs. (39) and (41) can be approximated by the simpler quantity $B_h/\sqrt{I_h}$. When the resonator's magnets make a significant contribution to the moment of inertia, optimization involves decreasing the size of the magnets to minimize I_h while keeping enough magnetic material to create a strong field B_h. For the design of Ref. 15, the optimization process reduced the magnets to the point where the elastic beam's contribution to the moment of inertia was twice that of the "magnetic sandwich." The resulting spin-resonator torque was smaller by a factor of four than the limiting value associated with Eq. (43). The figure of merit for the optimization was the single-shot SNR for a single-spin sample, as given by Eq. (15). The optimization was performed using the values $\tau_h = 6\ \mu$s, $T_{1\rho} = 1$ s, $D = 1$, $A = 1/2$, and $T_h = 10$ mK, with a minimal separation of 25 nm between the magnetic cylinders, and a minimal beam cross section of 50×50 nm.[15,46] The optimized design had a magnetic sandwich of height 105 nm and diameter 55 nm, with $\omega_h/2\pi = 630$ MHz. The rate constant for polarization between transients was $R_h = 1.3\ \text{s}^{-1}$. Since the value of $T_{1\rho}$ assumed for the optimization turned out to be $1.3/R_h$, which is similar to the limiting upper value of $2/R_h$ given by Eq. (34), sensitivity estimates obtained from the full SNR formula correspond fairly well to the values obtained from Eqs. (37) and (38). These simpler formulas are used in Sec. III C to characterize detection sensitivity under near-optimal conditions.

Since different types of mechanical motion were found to yield similar values of the coupling constant g,[46] the primary criteria used in selecting the design to be optimized were the absence of relative motion between the sample and the magnets and the homogeneity of the resonator's field at the spins. A practical resonator design would need to take account of additional criteria, such as constraints associated with the detection of the mechanical motion. Experimental tests would be needed for optimization.

It is informative to estimate the range of values that can be expected for

$$\omega_{\text{rd}} = R_0\,(PN/2). \tag{44}$$

As discussed in Sec. III A, this angular frequency is obtained from a simple macroscopic model of radiation damping. In considering the significance of system parameters for resonator design, we use ω_{rd} as a measure of the coupling between the sample and the resonator, since it quantifies in a simple way the net effect of changes in the sample size and the rate constant

$$R_0 = 2g^2\tau_h$$

when system parameters are varied.

The coupling constant g can be estimated from the resonator's dimensions and material properties to be $\sim 300\ \text{s}^{-1}$,[46] but τ_h cannot be accurately predicted. The assumption $\tau_h = 6\ \mu$s, discussed in Ref. 15, yields $R_0 \sim 1\ \text{s}^{-1}$. The Larmor frequency can be considered nearly resonant with the mechanical motion if $|\omega_0|$ differs from ω_h by no more than $1/\tau_h = 2\pi \times 25$ kHz. This frequency offset decreases the spectral density of the mechanical fluctuations at ω_0 by a factor of two, which decreases R_0 by the same factor.[14] Finite-element simulations showed that the resonant volume is a cylinder of height 1.4 nm and diameter 2 nm.[15] An ice sample filling this volume would contain $N \sim 300$ protons, and with $P \sim 1$, we obtain

$$\omega_{\text{rd}}/2\pi \sim 150\ \text{Hz}.$$

Scaling up the spin-resonator system would give a larger value of N in Eq. (44) but would be expected to decrease ω_{rd}, since g scales strongly with size. For example, uniform scaling

of the resonator gives

$$g^2 \propto \frac{1}{I_h \omega_h} \propto r^{-4},$$

where r is a characteristic resonator dimension.[14] In the regime where the magnetic sandwich makes the dominant contribution to the moment of inertia, the frequency can be adjusted independently of I_h by changes to the elastic beam. If the Larmor frequency is held constant during the scaling, so that P is preserved, we have

$$g^2 \propto \frac{1}{I_h} \propto r^{-5}.$$

Moving beyond the assumption that $\tau_h = 6\ \mu$s, we note that although a shorter τ_h would yield a larger resonant volume, the need to efficiently manipulate the spins with applied rf fields limits the frequency range that can be studied spectroscopically. The 50-kHz field inhomogeneity across the resonant volume for $\tau_h = 6\ \mu$s is a characteristic proton spectral width, and for this discussion, we treat it as a rough upper limit on the field inhomogeneity across the sample volume, independent of the value of τ_h. With this assumed constraint, a drop in τ_h below 6 μs causes a drop in R_0 without affecting the sample volume. An increase in τ_h above 6 μs gives an increase in R_0 but shrinks the resonant volume. For instance, $\tau_h = 60\ \mu$s gives $R_0 \sim 10\ \mathrm{s}^{-1}$ and a resonant spectral width of 5 kHz. An ice sample filling the resonant volume would contain about 10 protons, yielding $\omega_{\mathrm{rd}}/2\pi \sim 50$ Hz.

Although weak damping is advantageous for the development of strong spin-resonator correlations and the efficient transfer of quanta from the spins to the resonator during the polarization process, the damping must be sufficiently strong to dissipate quanta into the thermal bath before they can be cycled back to the spins. For a resonator at temperature $T_h = 0$ K, the condition

$$g\sqrt{N} \ll \frac{2}{\tau_h} \tag{45}$$

guarantees that the resonator causes spin relaxation rather than participating in a coherent exchange of quanta with the spins.[14,48] For the example with $\tau_h = 6\ \mu$s and $N = 300$, the left side of Eq. (45) is smaller than the right side by a factor of 60, while the ratio drops to 30 for the example with $\tau_h = 60\ \mu$s and $N = 10$. Note that at the estimated mechanical frequency of 630 MHz, a temperature of $T_h = 10$ mK gives $P = 0.9$ and $n_{\mathrm{th}} = 0.05$, which are close to the limiting values. For many purposes, the approximation $T_h \sim 0$ K can be used to characterize this frequency and temperature, and in particular, the use of Eq. (45) is justified.

For the polarization process, the edge of the resonant volume can be defined by the condition $|\omega_0| = \omega_h \pm 1/\tau_h$. However, for pulsed spin locking, the delay between pulses must be several multiples of τ_h, and so the range of spectral frequencies should be small compared to $1/\tau_h$. Direct driving of the resonator by the rf field can be minimized by applying the pulses along the length of the torsion beam, so that the torque exerted on the resonator by the field is orthogonal to the torque needed to drive torsional motion. However, a short ring-down time between pulses is a likely a practical requirement for detection of a spin-locked signal, due to unavoidable imperfections in the rf field and excitation of off-resonant mechanical modes.

These rough estimates illustrate the significance of size constraints associated with resonator fabrication. In particular, the coupling constant g and the volume of resonant spins both depend strongly on the size constraints chosen for the optimization. The resonant volume, with dimensions $\sim$1 nm, is a small fraction of the volume separating the two magnets, which is a cylinder of diameter 55 nm and height 25 nm. Although this is partly an artifact of having used single-spin sensitivity as the figure of merit for the optimization, it is true more generally that the separation between the magnets plays a key role in determining field homogeneity. The resonator's moment of inertia, which is responsible for the scaling properties of g, is limited by the constraint of a 50×50 nm cross section for the elastic beam. These size constraints were chosen to be roughly consistent with current fabrication capabilities, but they do not represent fundamental limits. Practical size constraints depend on fabrication technology that is under active development.

Implementation depends on the capability to manipulate the spins by means of rf fields without heating the resonator. At frequency 600 MHz, for example, the polarization is sensitive to temperature increases above 10 mK, dropping from 0.9 to 0.3 as the temperature increases to 50 mK, with $P \propto 1/T_h$ for continued temperature increases. Eddy currents in the resonator's magnetic material are a principal concern with regard to heating. Although a quantitative prediction of eddy-current heating in the size and temperature regime of interest is difficult, a rough estimate suggests the using low-conductivity material as the source of the resonator's field could render eddy-current heating insignificant.[15,46] EuO is promising for this purpose, since it has a large saturation magnetization and a low electrical conductivity at low temperatures,[49] and since methods of integrating it into microfabricated devices have been developed.[50]

The sensitivity of the motion detection is of critical importance for spectroscopic sensitivity, as illustrated by the numerical example presented in Sec. III C. The quantum-limited sensitivity for a single-spin sample is 1/3, while the measurement conditions described as "near-optimal" give $\rho/N = 0.07$. The difference between these two values is primarily due to the assumption that the noise associated with the near-optimal motion detector is equivalent to $A = 16$ thermal quanta in the resonator, rather than to the limiting value $A = 1/2$. In the regime where $P \sim 1$, the motion detector is likely to be the dominant noise source, since the noise associated with resonator fluctuations is nearly equal in magnitude to the noise added by a quantum-limited motion detector. Methods for detecting microscopic mechanical motion at temperatures below 100 mK with a sensitivity near the quantum limit have been demonstrated experimentally,[51] including capacitive measurement by means of a single-electron transistor.[43] For the resonator design we have discussed, detector geometries for capacitive motion detection have been proposed.[15] However, the problem of implementing sensitive motion detection for force-detected NMR in the relevant regime has not been studied in detail,[1] and substantial development is needed in this area.

Our focus in this paper has been the sensitivity of multidimensional methods in which an arbitrary evolution period is followed by optimized detection during a period of pulsed spin locking. One-dimensional spectroscopy with direct detection of free evolution is also possible. Of particular interest in this regard are single-molecule samples sufficiently small and isolated to yield resolved spectra. In the absence of line broadening due to a broad distribution of couplings and chemical shifts, the signal lifetime during free evolution is limited by resonator-induced dissipation and radiation damping, which become more significant with improvements in the resonator's efficiency. Although its applicability is limited by line broadening in larger samples, one-dimensional NMR spectroscopy could be used for systems of a few spins in the low-temperature regime.

V. CONCLUSION

Even if instrument noise is decreased near the level associated with the resonator's zero-point motion and with the quantum limit on motion detection, it is larger than spin noise for sufficiently small samples. In this regime, resonator-induced polarization of order unity would enhance spectroscopic detection sensitivity by an order of magnitude or more. More generally, under conditions where instrument noise dominates spin noise, polarizing the sample enhances the sensitivity of NMR spectroscopy if $P > \rho/PN$, that is, if P is larger than the SNR for detecting a fully-polarized spin during a single transient.

When the signal lifetime is limited by resonator-induced decay and the noise is associated with resonator fluctuations, a balance exists between the coupling strength, the noise power, and the signal lifetime. In the limiting case of ideal pulsed spin locking, the only parameter of the spin-resonator system that affects the sensitivity per spin is ω_h/T_h. Since the criterion for a classical description of the resonator to be valid is $\omega_h/T_h \ll k_B/\hbar$, near-optimal sensitivity occurs in the regime where departures from classical behavior are significant, with $n_{\rm th} < 1$ and $P \sim 1$.

An intrinsic sensitivity limit exists for resonant detection of a spin signal, due to the fact that the resonant interaction shortens the signal lifetime by enhancing the spins' spontaneous emission. When instrument noise is quantum limited and signal decay is due to spontaneous emission into the resonator, the SNR for detection of a single spin is $1/3$.

For implementation of force-detected NMR spectroscopy with resonator-induced polarization, the polarization time $\sim 1/R_h$ must be sufficiently short to allow for averaging over many transients. The delay between transients is minimized when the coupling constant g for the resonant interaction is large, and when the damping of the resonator is weak. Together these conditions allow for the buildup of strong spin-resonator correlations that efficiently transfer quanta from the spins to the resonator. However, a short resonator ring-down time is desirable for fast recovery during pulsed spin locking, for polarization of samples with broad spectra, and for fast dissipation of quanta transferred to the resonator. The magnitude of the coupling constant is therefore of key importance for resonator design. The achievable strength of the resonant interaction depends on practical size constraints, since g scales strongly with size.

Torsional resonators offer advantages for force-detected NMR. The interaction between the spins and the resonator does not depend on a gradient generated by the resonator's magnets or on relative motion between the sample and the magnets. As a result, the sample can in principle be placed arbitrarily close to the magnets without a problematic increase in damping, consistent with the design goal of a strong coupling constant. The lack of dependence on a gradient facilitates the optimization of field homogeneity, needed for the polarization and spectroscopy of samples containing many spins. The torque acting between the spins and the resonator is enhanced by the presence of a strong applied field that holds the resonator's magnetization motionless during the mechanical oscillations and yields a large thermal polarization at low temperatures. Analysis of a prototypical resonator design suggests that although substantial development is needed, resonator-induced polarization could enable NMR spectroscopy as a tool for studying low-temperature nanoscale samples, down to the single-spin limit.

APPENDIX A: SIGNAL PROCESSING

1. Detection of a polarized dipole

a. Filter definition

The sensitivity analysis in Sec. II A is based on an idealized signal-processing protocol in which the sum of the signal $s(t)$ and the noise $n(t)$,

$$y(t) = s(t) + n(t),$$

is passed through a time-invariant linear filter L. To motivate the definition of the filter, we consider the problem of analyzing the data acquired during ideal pulsed spin locking. If the signal lifetime $T_{1\rho}$ has been measured independently, the functional form of $s(t)$ is known. The data analysis should yield an estimate of $s(t_1)$, where time t_1 corresponds to the beginning of the detection period. As discussed in Sec. II A1, measurement of $s(t_1)$ yields a single point of an FID that follows an arbitrary pulse sequence.

The signal-processing scheme described here is based on the assumption that the functional form of $s(t)$ is known. A matched filter is used to measure $s(t_1)$, where t_1 represents the beginning of an arbitrary detection period. We write the signal torque

$$s(t) = \gamma\hbar \frac{dB_x}{d\theta} \langle I_x(t)\rangle$$

in the form

$$s(t) = G s_0(t), \tag{A1}$$

where

$$G = s(t_1) = \gamma\hbar \frac{dB_x}{d\theta} \langle I_x(t_1)\rangle \tag{A2}$$

is the quantity to be measured, formally analogous to a signal amplification or gain. The normalized signal $s_0(t)$ is defined by

$$s_0(t) = \frac{\langle I_x(t)\rangle}{\langle I_x(t_1)\rangle} \tag{A3}$$

for times $t > t_1$, with $s_0(t) = 0$ before the beginning of the detection period. For detection during ideal pulsed spin locking, we have

$$s_0(t) = \begin{cases} \cos[\omega_0(t-t_1)]\, e^{-(t-t_1)/T_{1\rho}}, & t \geqslant t_1, \\ 0, & t < t_1. \end{cases} \quad \text{(A4)}$$

The signal processing is performed by passing

$$y(t) = G s_0(t) + n(t)$$

through a normalized filter L, that is, a filter that produces output 1 at some known time t_0 in response to the input $s_0(t)$. Since we can consider the filter to be implemented using software, we set $t_0 = 0$ for convenience. Passing $y(t)$ through the normalized filter then gives

$$y_L(0) = G + n_L(0), \quad \text{(A5)}$$

where a subscript "L" has been used to indicate the output of the filter. The filter is designed to maximize the SNR ρ, which is defined by

$$\rho^2 = \frac{s_L^2(0)}{\langle n_L^2(0)\rangle} = \frac{G^2}{\langle n_L^2\rangle}. \quad \text{(A6)}$$

Note that in the second equality, we have assumed that $n(t)$ is a stationary random process, which implies that $\langle n_L^2\rangle$ does not depend on time.

In general, the transfer function of the optimum filter is determined by the Fourier transform of the signal and the spectral density of the noise.[52] In the case where the noise is white, the optimum choice is a matched filter that extracts the signal from the noise using only the Fourier components of $s_0(t)$.[52] In response to an input $f(t)$, the output of the filter at time $t_0 = 0$ is

$$f_L(0) = \frac{1}{E_0}\int_{-\infty}^{\infty} f(t)\, s_0(t)\, dt, \quad \text{(A7)}$$

where the normalization constant

$$E_0 = \int_{-\infty}^{\infty} s_0^2(t)\, dt \quad \text{(A8)}$$

can be interpreted as a measure of the energy in $s_0(t)$. In the case where $s_0(t)$ is given by Eq. (A4), we have

$$E_0 = \frac{T_{1\rho}}{4}. \quad \text{(A9)}$$

Note that when the signal and the spin fluctuations decay on the same time scale, the spectral density of the spin noise varies within the signal bandwidth. In the case where narrow-bandwidth spin noise is a significant noise source, a filter that takes account of the power spectrum of the spin noise would improve sensitivity. Our use of a matched filter for the sensitivity analysis is therefore best suited to the regime where the spin noise is small compared to broad-bandwidth instrument noise.

b. Instrument noise

The variance σ_n^2 introduced into the measurement by the filtered noise is

$$\sigma_n^2 = \langle n_L^2\rangle = \frac{1}{2\pi}\int_0^{\infty} |H(\omega)|^2\, S_n(\omega)\, d\omega, \quad \text{(A10)}$$

where $H(\omega)$ is the filter's transfer function and S_n is the spectral density of $n(t)$. In order to evaluate Eq. (A10), we note that

$$|H(\omega)|^2 = \frac{|s_0(\omega)|^2}{E_0^2},$$

where $s_0(\omega)$ is the Fourier transform of $s_0(t)$, defined by

$$s_0(\omega) = \int_{-\infty}^{\infty} e^{-i\omega t} s_0(t)\, dt.$$

Equation (A10) can thus be written in the form

$$\sigma_n^2 = \frac{1}{2\pi E_0^2}\int_0^{\infty} |s_0(\omega)|^2\, S_n(\omega)\, d\omega. \quad \text{(A11)}$$

In the case where spin noise is negligible, $n(t)$ can be identified with instrument noise, and Eq. (A11) gives

$$\sigma_{\text{inst}}^2 = \frac{1}{2E_0} S_{\text{inst}}, \quad \text{(A12)}$$

where S_{inst} is the spectral density of Eq. (9), evaluated at the mechanical frequency, and where σ_{inst}^2 represents the variance due to filtered instrument noise. Defining

$$\Delta\nu = \frac{1}{2E_0}, \quad \text{(A13)}$$

we write Eq. (A12) as

$$\sigma_{\text{inst}}^2 = S_{\text{inst}}\Delta\nu. \quad \text{(A14)}$$

For detection during ideal pulsed spin locking, the bandwidth is $\Delta\nu = 2/T_{1\rho}$, which gives

$$\sigma_{\text{inst}}^2 = \frac{2}{T_{1\rho}} S_{\text{inst}}. \quad \text{(A15)}$$

Since the resonator must in general ring down after a pulse before detecting the spin signal, it can only function as a detector during a fraction D of the detection period. We can take account of the duty cycle by replacing the normalized signal $s_0(t)$ of Eq. (A4) with a function that is switched to zero during the times when the resonator is not detecting a signal. The energy E_0 is decreased as a result of this change, and the bandwidth is multiplied by $1/D$:

$$\Delta\nu = \frac{2}{DT_{1\rho}}.$$

Assuming that the bandwidth of the instrument noise is broad compared to the Fourier transform of the switched signal, Eq. (A15) is then replaced by

$$\sigma_{\text{inst}}^2 = \frac{2}{DT_{1\rho}} S_{\text{inst}}. \quad \text{(A16)}$$

c. Spin noise

In Sec. II A3, we consider two methods of describing spin noise. For detection of N spins during pulsed spin locking, we model the fluctuations of the spin-locked component as a stationary random process that causes variation in the amplitude of the signal torque. The spectral density of the amplitude fluctuations is given by Eq. (13) as

$$S_{\text{spin}}(\omega) = N\left(\gamma\hbar\frac{dB_x}{d\theta}\right)^2 \frac{T_{1\rho}}{1+\omega^2 T_{1\rho}^2}.$$

The spin noise passed into the filter can be written in the form

$$n(t) = n^*(t)\cos(\omega_0 t),$$

where $n^*(t)$ represents the amplitude noise and where the beginning of the detection period has been set to $t_1 = 0$. With the normalized signal given by Eq. (A4), the filtered spin noise is

$$\begin{aligned} n_L(0) &= \frac{4}{T_{1\rho}}\int_0^\infty n^*(t)\cos^2(\omega_0 t)\, e^{-t/T_{1\rho}}\, dt \\ &\approx \frac{2}{T_{1\rho}}\int_0^\infty n^*(t) e^{-t/T_{1\rho}}\, dt. \end{aligned}$$

The arguments used in deriving Eq. (A11) can be adapted to show that the variance of the filtered spin noise is

$$\begin{aligned} \sigma_{\text{spin}}^2 &= \frac{1}{2\pi}\int_0^\infty \frac{4}{1+\omega^2 T_{1\rho}^2} S_{\text{spin}}(\omega)\, d\omega \\ &= \frac{N}{2}\left(\gamma\hbar\frac{dB_x}{d\theta}\right)^2. \end{aligned} \tag{A17}$$

A more rigorous approach to characterizing spin noise is to find the variance of the quantum-mechanical operator that corresponds to the filtered spin torque. If the input to the filter is the operator $T(t)$ of Eq. (4), which represents the torque exerted on the resonator by the spins, the filter output is given by

$$T_L = \gamma\hbar\frac{dB_x}{d\theta}\frac{1}{E_0}\int_{-\infty}^\infty I_x(t) s_0(t)\, dt \tag{A18}$$

$$\propto \int_{t_1}^\infty I_x(t)\,\langle I_x(t)\rangle\, dt, \tag{A19}$$

where the time argument of the filter output has been suppressed.

The significance of treating the filter output as an operator can be highlighted by considering the way in which Eq. (A5) is modified when the input $s(t)$ is replaced with $T(t)$. Passing the signal $s(t) = G s_0(t)$ into the filter yields the output G, and variance in the measurement is associated with filtered noise n_L. When the filter output is treated as an operator, the outcome of the measurement depends on the statistical properties of T_L. Equations (A2), (A3), (A8), and (A18) imply that

$$\langle T_L\rangle = G, \tag{A20}$$

but the variance of T_L represents a noise source, which can be identified with the filtered spin noise σ_{spin}^2:

$$\sigma_{\text{spin}}^2 = \langle T_L^2\rangle - \langle T_L\rangle^2. \tag{A21}$$

Substituting Eq. (A18) into Eq. (A21) gives

$$\begin{aligned} \sigma_{\text{spin}}^2 \propto \int_{t_1}^\infty\int_{t_1}^\infty &[\langle I_x(t) I_x(t')\rangle - \langle I_x(t)\rangle\langle I_x(t')\rangle] \\ &\times \langle I_x(t)\rangle\langle I_x(t')\rangle\, dt'\, dt, \end{aligned} \tag{A22}$$

which expresses σ_{spin}^2 as the output of a two-dimensional filter, with spin fluctuations characterized by

$$\langle I_x(t) I_x(t')\rangle - \langle I_x(t)\rangle\langle I_x(t')\rangle$$

as the filter input.

d. Discussion

Although we motivated the use of a matched filter by considering the problem of analyzing a spin-locked signal, the idealized method of signal analysis that we have discussed does not depend on an assumption that the detection period involves spin locking. Certain results derived here can therefore be applied to the example considered in Sec. III B, where a single-spin sample is detected during free precession. The normalized signal $s_0(t)$ used to define the matched filter is a sinusoid that decays exponentially with time constant T_2, and the measurement bandwidth is given by Eqs. (A8) and (A13) as

$$\Delta\nu = 2/T_2. \tag{A23}$$

From Eq. (A14), the instrument noise is

$$\sigma_{\text{inst}}^2 = (2/T_2) S_{\text{inst}}.$$

The spin noise, as defined by Eq. (A21), is evaluated in Appendix B.

The use of a matched filter for signal analysis is assumed throughout most of this paper, but Sec. III B extends the discussion to the case where the detailed functional form of the signal $s(t)$ is characterized by means of a set of sampled points, rather then being known in advance. The definition of SNR given by Eq. (A6) can be generalized to this case in a natural way. We define

$$\rho^2 = \sum_k \frac{s_L^2(t_k)}{\langle n_L^2\rangle}, \tag{A24}$$

where t_k ranges over the set of sampled points, and where the filter L depends on the spectral width and the details of the detection method. Note that Eq. (A24) implicitly depends on the assumption that the noise at different times t_k is independent. If the noise for different sampled points is correlated, then knowledge of the correlations could, in general, be used to increase the information extracted from the measurement, and the sensitivity would be underestimated by Eq. (A24). In the regime where the noise has a broad bandwidth, however, Eq. (A24) provides a measure of sensitivity which takes account of the energy in all Fourier components of the filtered signal that are within the sampled bandwidth. Equations (A6) and (A24) allow for rigorous comparison of detection schemes that measure a single value per shot and those that sample a continuous time-dependent function during each shot.

2. Detection of spin-noise correlations

The signal-processing protocol for detection of a polarized sample dipole can be adapted for detection of spin-noise correlations, which is discussed in Sec. II B. The signal and noise are defined as functions of two time-domain arguments:

$$y(t,t') = s(t,t') + n(t,t').$$

The signal corresponding to a single shot of the experiment is expressed in the form

$$s(t,t') = G s_0(t,t'),$$

where s_0 is a known function and G is the quantity to be measured. The filter L used to analyze $y(t,t')$ is defined by

$$f_L = \frac{1}{E_0}\int_{-\infty}^{\infty}\int_{-\infty}^{\infty} f(t,t')s_0(t,t')\,dt\,dt', \tag{A25}$$

where

$$E_0 = \int_{-\infty}^{\infty}\int_{-\infty}^{\infty} s_0^2(t,t')\,dt\,dt'. \tag{A26}$$

As in Eq. (A6), the single-shot SNR ρ is defined by

$$\rho^2 = \frac{s_L^2}{\langle n_L^2\rangle} = \frac{G^2}{\langle n_L^2\rangle}. \tag{A27}$$

In Appendix C, we use Eqs. (A25) through (A27) to analyze the sensitivity of the CONQUEST detection scheme.

APPENDIX B: FILTERED SPIN NOISE

In this Appendix, we evaluate the filtered spin noise $\sigma_{\rm spin}^2$ for the single-spin example discussed in Sec. III B. We also derive a differential equation that illustrates the dependence of $\sigma_{\rm spin}^2$ on the details of the internal spin Hamiltonian $H_{\rm int}$ for detection of N spins during pulsed spin locking.

As discussed in Sec. II A 3 and Appendix A 1, filtered spin noise is associated with quantum-statistical uncertainty in the operator that corresponds to the filtered signal. The variance in the measurement due to spin noise is given by Eq. (A21) as

$$\sigma_{\rm spin}^2 = \langle T_L^2\rangle - \langle T_L\rangle^2,$$

where T_L is defined by Eq. (A18). From Eqs. (A2) and (A20), we obtain

$$\langle T_L\rangle = \gamma\hbar\frac{dB_x}{d\theta}\langle I_x(0)\rangle, \tag{B1}$$

where time t_1, the beginning of the detection period, has been set to zero. In order to find $\langle T_L^2\rangle$, we must obtain an expression for the correlation function

$$C_I(t,t') = \langle I_x(t)I_x(t') + I_x(t')I_x(t)\rangle, \tag{B2}$$

since

$$\langle T_L^2\rangle \propto \int_0^{\infty}\int_0^{t} C_I(t,t')\langle I_x(t)\rangle\langle I_x(t')\rangle\,dt'\,dt. \tag{B3}$$

We first consider the example where a spin 1/2 initially aligned with the x axis is detected during free precession. The quantum regression formula[35] can be used to evaluate $C_I(t,t')$. The master equation is

$$\frac{d\sigma}{dt} = -i\,[\omega_0 I_z,\sigma] + \Lambda\sigma, \tag{B4}$$

where the relaxation superoperator Λ is given by Eq. (25). Using Eq. (B4) in the quantum regression formula in combination with the identities

$$I_x^2 = 1/4, \quad I_xI_y + I_yI_x = 0,$$

gives

$$C_I(t,t') = \tfrac{1}{2}\cos(\omega_0|t-t'|)e^{-|t-t'|/T_2}.$$

From Eq. (A18), we obtain

$$\langle T_L^2\rangle = \frac{1}{2}\left(\gamma\hbar\frac{dB_x}{d\theta}\frac{4}{T_2}\right)^2\int_0^{\infty}\int_0^{t}\cos[\omega_0(t-t')] \times\cos(\omega_0 t)\cos(\omega_0 t')e^{-2t/T_2}\,dt'\,dt,$$

which evaluates to

$$\langle T_L^2\rangle = \frac{1}{2}\left(\gamma\hbar\frac{dB_x}{d\theta}\right)^2. \tag{B5}$$

Equations (B1) and (B5) then give

$$\sigma_{\rm spin}^2 = \langle T_L^2\rangle - \langle T_L\rangle^2 = \frac{1}{4}\left(\gamma\hbar\frac{dB_x}{d\theta}\right)^2. \tag{B6}$$

For detection of N spins during ideal pulsed spin locking, Eq. (35) can be used to study the decay of correlations in the toggling frame. We find that for $t' > t$,

$$\langle I_x(t)I_x(t')\rangle = \langle I_x^2(t)\rangle e^{-(t'-t)/T_{1\rho}}, \tag{B7}$$

where $T_{1\rho} = 2/R_h$. The equation of motion for $\langle I_x^2(t)\rangle$ in the toggling frame is

$$\frac{d}{dt}\langle I_x^2(t)\rangle = -R_h\langle I_x^2(t)\rangle + R_h\left[a^2\langle I_z^2(t)\rangle + b^2\langle I_y^2(t)\rangle\right], \tag{B8}$$

where $a^2 + b^2 = 1$.

Equation (B8) shows that resonator-induced transitions cause the decay of $\langle I_x^2(t)\rangle$ while simultaneously converting $\langle I_y^2(t)\rangle$ and $\langle I_z^2(t)\rangle$ to $\langle I_x^2(t)\rangle$. Since the equations of motion for $\langle I_y^2(t)\rangle$ and $\langle I_z^2(t)\rangle$ include coherent evolution under the time-averaged Hamiltonian $\bar{H}_{\rm int}$, the details of the internal Hamiltonian play an essential role in determining the evolution of $\langle I_x^2(t)\rangle$ during spin locking. Rather than doing a detailed study of this evolution, we have based the sensitivity analysis on a simplified model of spin noise in which the fluctuations of an unpolarized sample are superimposed on the spin-locked component. The resulting estimate of $\sigma_{\rm spin}^2$ is given by Eq. (A17).

APPENDIX C: SIGNAL-TO-NOISE RATIO FOR DETECTION OF SPIN-NOISE CORRELATIONS

In this Appendix we derive Eq. (21), the sensitivity formula for detection of spin-noise correlations. Since the spin system is assumed to be completely disordered before the measurement is performed, the density matrix is proportional to the identity throughout the measurement process. For simplicity, the evolution of $I_x(t)$ during the time period of spectroscopic interest is assumed to be given by

$$I_x(t_1) = I_x\cos(\omega t_1) + I_y\sin(\omega t_1), \tag{C1}$$

as in the derivation of Eq. (18).

We wish to use the signal-processing scheme described in Appendix A 2 for the sensitivity analysis. We therefore begin by expressing the signal

$$s(t,t') = \left(\gamma\hbar\frac{dB_x}{d\theta}\right)^2\langle I_x(t)I_x(t')\rangle$$

in the form

$$s(t,t') = Gs_o(t,t'),$$

where $s_0(t,t')$ is a known function. This is done by using the quantum regression formula,[35] in combination with some simplifying assumptions, to evaluate the correlation function

$$R_I(t,t') = \langle I_x(t)I_x(t')\rangle.$$

The evolution period from $t = 0$ to $t = t_1$ is assumed to be short on the time scale of spin fluctuations. In evaluating $R_I(t,t')$, we approximate the evolution that occurs during this period as an instantaneous rotation of the operator $I_x(t)$ through an angle $\phi = \omega t_1$, consistent with the fact that Eq. (C1) includes no relaxation. The physical quantity of interest in the measurement is the value of ϕ, since it carries information about the spectral frequency ω.

In the toggling frame where the Hamiltonian for the rf field has been eliminated, the master equation is given by Eq. (35). Application of the quantum regression formula shows that correlations in the spin-locked component decay exponentially with time constant $T_{1\rho}$ in this frame, as described by Eq. (B7), with $\langle I_x^2(t)\rangle = N/4$ for the disordered system. The other spin components in general decay quickly during spin locking, and we assume that laboratory-frame correlation functions for transverse spin components can be obtained from Eq. (B7) simply by taking account of the rotation about the z axis that occurs in the laboratory frame. When $t,t' < 0$, this approximation gives

$$R_I(t,t') = \frac{N}{4}\cos(\omega_0 t)\cos(\omega_0 t')e^{-|t-t'|/T_{1\rho}}. \qquad \text{(C2)}$$

When $t > t_1$ and $t' < 0$, we obtain

$$R_I(t,t') = \frac{N}{4}\cos\phi\,\cos[\omega_0(t-t_1)]\cos(\omega_0 t')e^{-(t-t')/T_{1\rho}}. \qquad \text{(C3)}$$

Note that Eq. (C2) does not depend on ϕ and thus carries no physical information for the measurement. Similarly, at times (t,t') for which $t,t' < 0$ or $t,t' > t_1$, the data $y(t,t')$ does not carry any information about the correlation to be measured, and the analysis is simplified if we set y to zero at these points. An additional simplification can be made by noting that

$$y(t,t') = T_{\rm obs}(t)T_{\rm obs}(t') = y(t',t).$$

Since the data $y(t,t')$ is identical in quadrants II and IV of the plane, there is no loss of information if we set y to zero in quadrant II and restrict the analysis to points in quadrant IV, where $t > 0$ and $t' < 0$. Finally, we assume that the torques observed during the short time period from $t = 0$ to $t = t_1$ are insignificant. We thus redefine the data $y(t,t')$ to exclude this time period:

$$y(t,t') = \begin{cases} T_{\rm obs}(t+t_1)\,T_{\rm obs}(t'), & t \geqslant 0, t' \leqslant 0, \\ 0, & \text{otherwise.} \end{cases}$$

The signal $s(t,t')$ can then be expressed as $Gs_0(t,t')$, where

$$G = \langle T(t_1)T(0)\rangle = \left(\gamma\hbar\frac{dB_x}{d\theta}\right)^2\frac{N}{4}\cos\phi, \qquad \text{(C4)}$$

and where

$$s_0(t,t') = \begin{cases} \cos(\omega_0 t)\cos(\omega_0 t')e^{-(t-t')/T_{1\rho}}, & t \geqslant 0, t' \leqslant 0, \\ 0, & \text{otherwise.} \end{cases}$$

The filter L of Eq. (A25) is used to extract an estimate of G from the noisy data. The variance introduced into the measurement by the instrument noise is $\langle n_L^2\rangle$, where

$$n_L = \frac{4}{T_{1\rho}}\int_0^\infty N_{\rm inst}(t)\cos(\omega_0 t)e^{-t/T_{1\rho}}\,dt \times \frac{4}{T_{1\rho}}\int_{-\infty}^0 N_{\rm inst}(t')\cos(\omega_0 t')e^{t'/T_{1\rho}}\,dt'. \qquad \text{(C5)}$$

The two integrals in Eq. (C5) are statistically independent, since the noise at time $t > 0$ is not correlated with the noise at time $t < 0$. We can thus evaluate $\langle n_L^2\rangle$ by finding the variance of each integral individually and then taking the product. Note that the normalization constant defined by Eq. (A26), $E_0 = T_{1\rho}^2/16$, has been split into two factors of $T_{1\rho}/4$, which separately normalize the two integrals in Eq. (C5). Each of the normalized integrals is equal to the filtered instrument noise for the first-order method in which a polarized dipole is detected. The variance of each integral is therefore given by Eq. (A15) as $(2/T_{1\rho})S_{\rm inst}$, and we find that

$$\langle n_L^2\rangle = \left(\frac{2}{T_{1\rho}}S_{\rm inst}\right)^2.$$

From Eq. (A27), the SNR is $|G|/\sqrt{\langle n_L^2\rangle}$, where G is given by Eq. (C4):

$$\rho_2 = N\,|\cos\phi|\,\frac{(\gamma\hbar/2)^2\,(dB_x/d\theta)^2}{(2/T_{1\rho})S_{\rm inst}}.$$

Setting $\cos\phi = 1$ yields the SNR formula of Eq. (21).

APPENDIX D: TIME AVERAGE OF THE RELAXATION SUPEROPERATOR

Section III A analyzes signal damping during pulsed spin locking and shows that if the internal Hamiltonian $H_{\rm int}$ and the relaxation superoperator Λ are averaged by the applied rf field, then $T_{1\rho} = 2/R_h$. This result depends on Eq. (31), which gives the time average of the toggling-frame superoperator $\tilde{\Lambda}$ during pulsed spin locking. Equation (31) is derived in this Appendix.

For simplicity, we assume that $\phi_p = 2\pi/n$ for some integer $n \geqslant 2$, which implies that the period of $\tilde{\Lambda}$ is $T_p = 2\pi/\bar{\omega}_1$. We also limit the discussion to the problem of calculating the time average of the term

$$A = \tilde{I}_+\tilde{\sigma}\,\tilde{I}_-$$

over the period T_p, since the analysis is similar for the other terms appearing in $\tilde{\Lambda}$. The frequency $\bar{\omega}_1$ is assumed to be sufficiently large that $\tilde{\sigma}$ can be considered constant during the period T_p.

Note first that

$$\tilde{I}_\pm(t) = I_x \pm i\,\tilde{I}_y(t),$$

since $\tilde{I}_x = I_x$. We thus have

$$A(t) = I_x\,\tilde{\sigma}\,I_x + i\tilde{I}_y(t)\,\tilde{\sigma}\,I_x - i\,I_x\,\tilde{\sigma}\,\tilde{I}_y(t) + \tilde{I}_y(t)\,\tilde{\sigma}\,\tilde{I}_y(t).$$

If the spin locking were continuous rather than pulsed, $\tilde{I}_y(t)$ would be given by

$$\tilde{I}_y(t) = \cos(-\omega_1 t) I_y + \sin(-\omega_1 t) I_z.$$

During pulsed spin locking, we instead have

$$\tilde{I}_y(t) = \cos[\phi(t)]\, I_y + \sin[\phi(t)]\, I_z,$$

where

$$\phi(t) = -\int_0^t \omega_1(t')\, dt'.$$

Note that if $\tilde{I}_y(t)$ is visualized as a vector rotating in the yz plane, then $\phi(t)$ is the angle between this vector and the y axis. Under the assumption that the modulation cycle consists of a square pulse followed by a delay, it is straightforward to verify that the time averages of $\cos[\phi(t)]$ and $\sin[\phi(t)]$ are both zero. In particular, the average of $\tilde{I}_y(t)$ over the delays is shown to be zero by means of the identity

$$\sum_{k=0}^{n-1} \exp(ik\phi_p) = \sum_{k=0}^{n-1} \exp[ik(2\pi/n)] = 0.$$

It follows that the time average of $A(t)$ can be written as

$$\bar{A} = I_x\, \tilde{\sigma}\, I_x + \frac{1}{T_p}\int_0^{T_p} \tilde{I}_y(t)\, \tilde{\sigma}\, \tilde{I}_y(t)\, dt. \qquad \text{(D1)}$$

To evaluate the integral in Eq. (D1), we expand the integrand as

$$\tilde{I}_y(t)\, \tilde{\sigma}\, \tilde{I}_y(t) = \cos^2[\phi(t)]\, I_y\, \tilde{\sigma}\, I_y + \sin^2[\phi(t)]\, I_z\, \tilde{\sigma}\, I_z + \cos[\phi(t)]\, \sin[\phi(t)]\, (I_y\, \tilde{\sigma}\, I_z + I_z\, \tilde{\sigma}\, I_y)$$

and let a^2 and b^2 denote the time averages of $\cos^2[\phi(t)]$ and $\sin^2[\phi(t)]$, respectively. Since $\cos^2\phi + \sin^2\phi = 1$, we have

$$a^2 + b^2 = 1.$$

Since the time average of

$$\cos[\phi(t)]\, \sin[\phi(t)] = \tfrac{1}{2}\sin[2\phi(t)]$$

is zero, Eq. (D1) simplifies to the form

$$\bar{A} = I_x\, \tilde{\sigma}\, I_x + a^2 I_y\, \tilde{\sigma}\, I_y + b^2 I_z\, \tilde{\sigma}\, I_z.$$

Using similar arguments to find the time average of the other terms appearing in $\tilde{\Lambda}$ yields Eq. (31).

*Present address: William R. Wiley Environmental Molecular Sciences Laboratory, Pacific Northwest National Laboratory, Richland, Washington 99352; mrkcbutler@gmail.com

[1] M. Poggio and C. L. Degen, Nanotechnology **21**, 342001 (2010).
[2] S. Kuehn, S. A. Hickman, and J. A. Marohn, J. Chem. Phys. **128**, 052208 (2008).
[3] J. A. Sidles, J. L. Garbini, K. J. Bruland, D. Rugar, O. Zuger, S. Hoen, and C. S. Yannoni, Rev. Mod. Phys. **67**, 249 (1995).
[4] C. L. Degen, M. Poggio, H. J. Mamin, C. T. Rettner, and D. Rugar, Proc. Natl. Acad. Sci. USA **106**, 1313 (2009).
[5] C. L. Degen, Q. Lin, A. Hunkeler, U. Meier, M. Tomaselli, and B. H. Meier, Phys. Rev. Lett. **94**, 207601 (2005).
[6] R. Joss, I. T. Tomka, K. W. Eberhardt, J. D. van Beek, and B. H. Meier, Phys. Rev. B **84**, 104435 (2011); K. W. Eberhardt, C. L. Degen, A. Hunkeler, and B. H. Meier, Angew. Chem. Int. Ed. **47**, 8961 (2008).
[7] M. Poggio, H. J. Mamin, C. L. Degen, M. H. Sherwood, and D. Rugar, Phys. Rev. Lett. **102**, 087604 (2009).
[8] K. W. Eberhardt, Q. Lin, U. Meier, A. Hunkeler, and B. H. Meier, Phys. Rev. B **75**, 184430 (2007); Q. Lin, C. L. Degen, M. Tomaselli, A. Hunkeler, U. Meier, and B. H. Meier, Phys. Rev. Lett. **96**, 137604 (2006).
[9] R. Verhagen, A. Wittlin, C. W. Hilbers, H. van Kempen, and A. P. M. Kentgens, J. Am. Chem. Soc. **124**, 1588 (2002).
[10] G. M. Leskowitz, L. A. Madsen, and D. P. Weitekamp, Solid State Nucl. Mag. **11**, 73 (1998).
[11] L. A. Madsen, G. M. Leskowitz, and D. P. Weitekamp, Proc. Natl. Acad. Sci. USA **101**, 12804 (2004).
[12] J. A. Sidles, Appl. Phys. Lett. **58**, 2854 (1991).
[13] P. L. Kuhns, P. C. Hammel, O. Gonen, and J. S. Waugh, Phys. Rev. B **35**, 4591 (1987).
[14] M. C. Butler and D. P. Weitekamp, Phys. Rev. A **84**, 063407 (2011).
[15] M. C. Butler, V. A. Norton, and D. P. Weitekamp, Phys. Rev. Lett. **105**, 177601 (2010).
[16] C. L. Degen, M. Poggio, H. J. Mamin, and D. Rugar, Phys. Rev. Lett. **99**, 250601 (2007); H. J. Mamin, R. Budakian, B. W. Chui, and D. Rugar, *ibid.* **91**, 207604 (2003).
[17] D. Rugar, R. Budakian, H. J. Mamin, and B. W. Chui, Nature (London) **430**, 329 (2004).
[18] S. A. Crooker, D. G. Rickel, A. V. Balatsky, and D. L. Smith, Nature (London) **431**, 49 (2004).
[19] J. Schlagnitweit, J.-N. Dumez, M. Nausner, A. Jerschow, B. Elena-Herrmann, and N. Müller, J. Magn. Reson. **207**, 168 (2010); M. Nausner, J. Schlagnitweit, V. Smrečki, X. Yang, A. Jerschow, and N. Müller, *ibid.* **198**, 73 (2009).
[20] G. M. Leskowitz, Ph.D. thesis, California Institute of Technology, 2003.
[21] L. A. Madsen, Ph.D. thesis, California Institute of Technology, 2002.
[22] P. J. Carson, L. A. Madsen, G. Leskowitz, and D. P. Weitekamp, US Patents No. 6078872 and 6081119 (2000).
[23] M. C. Butler and D. P. Weitekamp, Phys. Rev. B **85**, 104405 (2012).
[24] B. W. Shore and P. L. Knight, J. Mod. Opt. **40**, 1195 (1993).
[25] S. Haroche, in *New Trends in Atomic Physics*, edited by G. Grynberg and R. Stora, Proceedings of Les Houches Summer School of Theoretical Physics, XXXVIII, 1982 (Elsevier Science, Amsterdam, 1984), pp. 195–309.
[26] J. A. Sidles and D. Rugar, Phys. Rev. Lett. **70**, 3506 (1993).
[27] J. S. Waugh and C. H. Wang, Phys. Rev. **162**, 209 (1967); E. D. Ostroff and J. S. Waugh, Phys. Rev. Lett. **16**, 1097 (1966).
[28] W. K. Rhim, D. P. Burum, and D. D. Elleman, Phys. Rev. Lett. **37**, 1764 (1976).
[29] D. P. Weitekamp, Adv. Magn. Reson. **11**, 111 (1983).
[30] J. Baum and A. Pines, J. Am. Chem. Soc. **108**, 7447 (1986).
[31] K. Schmidt-Rohr, K. Saalwächter, S.-F. Liu, and M. Hong, J. Am. Chem. Soc. **123**, 7168 (2001); M. Hong and S. Yamaguchi, J. Magn. Reson. **150**, 43 (2001); Y. Ishii, J. P. Yesinowski, and R. Tycko, J. Am. Chem. Soc. **123**, 2921 (2001).

[32] A. T. Petkova and R. Tycko, J. Magn. Reson. **155**, 293 (2002).
[33] W. H. Louisell, *Quantum Statistical Properties of Radiation* (Wiley-Interscience, New York, 1990), Chap. 7; M. Lax, Phys. Rev. **145**, 110 (1966).
[34] G. W. Ford, J. T. Lewis, and R. F. O'Connell, Phys. Rev. A **37**, 4419 (1988); G. W. Ford and M. Kac, J. Stat. Phys. **46**, 803 (1987).
[35] G. W. Ford and R. F. O'Connell, Opt. Commun. **179**, 451 (2000).
[36] A. A. Clerk, Phys. Rev. B **70**, 245306 (2004).
[37] C. M. Caves, Phys. Rev. D **26**, 1817 (1982).
[38] F. Bloch, Phys. Rev. **70**, 460 (1946).
[39] M. M. Maricq, Phys. Rev. B **25**, 6622 (1982).
[40] A. Abragam, *Principles of Nuclear Magnetism* (Clarendon Press, Oxford, 1961), pp. 72–75.
[41] F. H. Allen, Acta Crystallogr. Sect. B **58**, 380 (2002).
[42] Our sensitivity analysis is based on the Langevin equation given by Eq. (3), which we derived by approximating the Hamiltonian $-\gamma \mathbf{I} \cdot \mathbf{B}(\theta)$ to first order in θ. The same equation can be derived when the interaction Hamiltonian is a weak perturbation of the form H_1, with $\omega_h = |\omega_0|$.
[43] M. D. LaHaye, O. Buu, B. Camarota, and K. C. Schwab, Science **304**, 74 (2004).
[44] J. L. Dormann, D. Fiorani, and E. Tronc, in *Advances in Chemical Physics*, edited by I. Prigogine and S. A. Rice, Vol. 98 (Wiley & Sons, New York, 2007), pp. 283–494; C. Kittel, Phys. Rev. **70**, 965 (1946).
[45] B. D. Cullity, *Introduction to Magnetic Materials* (Addison-Wesley, Reading, MA, 1972).
[46] M. C. Butler, Ph.D. thesis, California Institute of Technology, 2008.
[47] H. Chang, Br. J. Appl. Phys. **12**, 160 (1961).
[48] R. Bonifacio, P. Schwendiman, and F. Haake, Phys. Rev. A **4**, 302 (1971).
[49] A. Mauger and C. Godart, Phys. Rep. **141**, 51 (1986); Y. Shapira, S. Foner, and T. B. Reed, Phys. Rev. B **8**, 2299 (1973); B. T. Matthias and R. M. Bozorth, Phys. Rev. Lett. **7**, 160 (1961).
[50] A. G. Swartz, J. Ciraldo, J. J. I. Wong, Y. Li, W. Han, T. Lin, S. Mack, J. Shi, D. D. Awschalom, and R. K. Kawakami, Appl. Phys. Lett. **97**, 112509 (2010); A. Schmehl, V. Vaithyanathan, A. Herrnberger, S. Thiel, C. Richter, M. Liberati, T. Heeg, M. Rockerath, L. F. Kourkoutis, S. Muhlbauer, P. Boni, D. A. Muller, Y. Barash, J. Schubert, Y. Idzerda, J. Mannhart, and D. G. Schlom, Nat. Mater. **6**, 882 (2007); J. Lettieri, V. Vaithyanathan, S. K. Eah, J. Stephens, V. Sih, D. D. Awschalom, J. Levy, and D. G. Schlom, Appl. Phys. Lett. **83**, 975 (2003).
[51] C. A. Regal, J. D. Teufel, and K. W. Lehnert, Nat. Phys. **4**, 555 (2008); S. Etaki, M. Poot, I. Mahboob, K. Onomitsu, H. Yamaguchi, and H. S. J. van der Zant, *ibid.* **4**, 785 (2008).
[52] L. A. Wainstein and V. D. Zubakov, *Extraction of Signals from Noise* (Dover, New York, 1962).
[53] W. Davenport and W. Root, *An Introduction to the Theory of Random Signals and Noise* (McGraw-Hill, New York, 1958), Chap. 11.
[54] L. Zadeh and J. Ragazzini, Proc. IRE **40**, 1223 (1952).